Impact of bubble characteristics and particle properties on the fluid dynamics of an ebullated bed hydroprocessor

Valois Parisien

Thesis submitted to the
Faculty of Graduate and Postdoctoral Studies
in partial fulfilment of the requirement for the degree of
Master of Applied Science in Chemical Engineering

Department of Chemical and Biological Engineering
Faculty of Engineering
University of Ottawa

Abstract

Commercial ebullated bed hydroprocessors, such as the LC-Finer[SM], are used for the production of synthetic crude oil by upgrading bitumen extracted from the Canadian oil sands. The objectives of this thesis were to experimentally determine bubble characteristics at industrially relevant operating conditions for the design and optimization of the reactor's recycle pan, as well as to investigate the impact of a catalyst density distribution on the reactor's fluidization behaviour. High gas holdups have been reported for this type of industrial unit. As a result, high gas holdup conditions were required to assess the commercial unit fluid dynamics.

Industrial conditions for the bubble characteristics in the reactor freeboard were simulated in a high pressure gas-liquid bubble column operating at 6.5 MPa using nitrogen and a 0.5 wt.% aqueous ethanol solution. Local bubble characteristics, including gas holdups, bubble rise velocities, and chord lengths, were investigated under various operating conditions using a novel monofibre optical probe designed for high gas holdup and elevated pressure. High gas holdups were achieved (up to 60%) and relatively narrow chord length distributions were observed, where 90% of the bubbles diameters were 1.0 mm or less. The energy dissipated through the distributor plate was shown to have a significant impact on the initial bubble size generated and high gas holdups were also achieved at atmospheric pressure by varying the open-surface area of the distributor.

As a result, the impact of a catalyst density distribution on local fluidization behaviour was investigated at atmospheric pressure using the previously designed high energy dissipation gas-liquid distributor plate and a 0.5 wt.% aqueous ethanol solution. Commercial spent hydroprocessing catalysts having a relatively wide density distribution was used. The introduction of gas greatly impacted the fluidized bed dynamic by rendering the bed-freeboard interface diffuse at low superficial liquid velocity. Bed interface fluctuations were significantly reduced at elevated liquid flow rate due to average bubble size reduction caused by high shearing through the gas-liquid distributor plate. Solid holdup was most affected by the density distribution where bed expansion/contraction was dependent of the liquid flow rate due to varying particle-bubble dynamics.

Résumé

Les hydroprocesseurs à lit fluidisé triphasé commerciaux, tels que le LC-Finer^{MD}, sont utilisés pour la production de pétrole brut synthétique par la valorisation du bitume extrait des sables bitumineux canadiens. Les objectifs de cette thèse étaient de déterminer expérimentalement les caractéristiques de bulles à des conditions d'opération industriellement pertinentes pour la conception et l'optimisation de la cuve de recyclage du réacteur, ainsi que d'étudier l'impact d'une distribution de densité de catalyseur sur le comportement de fluidisation du réacteur. Des rétentions de gaz élevées ont été rapportées pour ce type d'unité industrielle. Par conséquent, des conditions d'opération menant à de haute rétention de gaz ont été nécessaires pour évaluer la dynamique des fluides de l'unité commerciale.

Les conditions industrielles pour les caractéristiques de bulle au-dessus du lit ont été simulées dans une colonne à bulles haute pression opérant à 6.5 MPa en utilisant de l'azote et une solution aqueuse de 0.5 %m d'éthanol. Les caractéristiques de bulles locales, y compris les rétentions de gaz, vitesses de montée de bulle, et les longueurs de corde, ont été étudiées à diverses conditions d'opération en utilisant une nouvelle sonde optique à monofibre conçu pour des rétentions de gaz et pressions élevées. Des rétentions de gaz élevées ont été obtenus (jusqu'à 60%) et des distributions de longueur de corde relativement étroites ont été observés, où 90% des bulles ont un diamètre de 1,0 mm ou moins. Il a été démontré que l'énergie dissipée au travers de la plaque distributrice gaz-liquide avait un impact significatif sur la taille des bulles initialement générés et des rétentions de gaz élevées ont également été réalisées à pression atmosphérique en variant la surface ouverte à l'écoulement du distributeur.

En conséquence, l'impact d'une distribution de densité de catalyseur sur le comportement de fluidisation locale a été étudié à pression atmosphérique en utilisant la plaque distributrice précédemment conçu ayant une énergie dissipée élevée et une solution aqueuse de 0.5 %m d'éthanol. Du catalyseur d'hydrotraitement usé ayant une relativement grande distribution de densité a été utilisé. L'introduction de gaz a impacté significativement la dynamique du lit fluidisé en rendant l'interface du lit diffuse à basse vitesse superficielle de liquide. Les fluctuations de l'interface du lit ont été réduites de manière significative à débit de liquide élevée due à la réduction de la taille moyenne des bulles causée par un taux de cisaillement élevé au travers de la plaque distributrice gaz-liquide. La rétention du solide a été la plus affectée par la

distribution de densité où l'expansion/contraction du lit était dépendante du débit de liquide en raison des variations de la dynamique particules-bulles.

Statement of Contributions of Collaborators

I hereby declare that I am the sole author of this thesis. I have performed the experimental studies and subsequent data analysis and I have written all of the chapters contained in this thesis.

My supervisor, Dr. Arturo Macchi, and industrial collaborators, Craig McKnight and Jason Wiens from Syncrude Canada Ltd., provided continual support and guidance throughout this work. They also contributed with many helpful editorial comments and corrections.

Experiments related to the paper presented in Chapter 2 were performed with the help of Alixia Farrell during the summer of 2014. She is a coauthor to the paper.

Dr. Dominic Pjontek provided guidance for the experimental work and contributed with editorial comments and corrections to Chapter 2 and Chapter 3. He is a coauthor to both papers.

Acknowledgments

I would first like to express my sincere gratitude to my supervisor, Dr. Arturo Macchi, for giving me the opportunity to work on this project and for his continuous support, guidance and inspiration throughout my graduate studies. His mentorship helped me believing in myself and made me the person I am today.

I would like to thank Syncrude Canada Ltd. for believing in this project and for their generosity in sponsoring the work. I would like to particularly thank Craig McKnight and Jason Wiens from Syncrude Canada Ltd. for their insight, support and guidance throughout this research program.

I would like to sincerely thank my research group colleagues Dr. Dominic Pjontek for his constant guidance and support for both experimental studies, Alixia Farrell for her assistance during experiments and various research tasks related to the local bubble characteristics study, and Chris Lane and Adam Donaldson for sharing their many inputs which helped improve further the fundamental analysis on the local bubble characteristics study.

I would also like to thank the technical staff in the Department of Chemical and Biological Engineering, Louis Tremblay, Franco Ziroldo and Gérard Nina, for their assistance during the many experimental systems maintenance and guidance for continual improvement.

I am very grateful to my fellow friends and classmates for their support and for making the work environment amusing. Lastly, I would like to thank my family, particularly my girlfriend Kristine Auprix, my parents Jean and Guylaine Parisien, and my sister Julianne Parisien, for their constant love and support during my studies.

Dedication

À Julianne (1993 – 2014)

Table of Contents

List of Figures

List of Tables

1 Introduction

Three-phase fluidized bed reactors are employed in industrial applications, such as catalytic hydroprocessing of heavy oil residues, Fischer-Tropsch synthesis, coal liquefaction, and waste water treatment (Fan, 1989), where intimate contact between gas, liquid and solid phases is crucial, resulting in excellent heat and mass transfer characteristics. Most research on gas-liquid-solid fluidized beds have been performed under ambient operating conditions using single-component liquids (Wild and Poncin, 1996). However, the unit of interest for this thesis is an ebullated bed hydroprocessor which operates at elevated temperatures and pressures and contains a multi-component liquid, resulting in complex fluid dynamic behaviour.

1.1 Synthetic crude oil production via bitumen upgrading in Canada

Canada has one of the largest oil reserves in the world, recently estimated at 168 billion barrels in the oil sands which are recoverable using currently available technology (Ancheyta and Speight, 2007; CAPP, 2014). Oil sand is composed of sand, bitumen, mineral rich clay and water. Once extracted, bitumen is a highly viscous and tar-like liquid which requires upgrading for transportation and conventional oil refining.

The Syncrude Project is a joint venture between a consortium of seven companies which produces synthetic crude oil through mining, extraction and upgrading of bitumen from the Athabasca oil sands. During the upgrading process, bitumen is distilled at near atmospheric pressures into light gas oil and atmospheric tower bottoms (ATB). A portion of the ATB is sent to a second distillation tower operating under vacuum pressures, further separating into light and heavy gas oils as well as the remaining vacuum tower bottoms (VTB). The ATB and VTB are in part upgraded via hydrogen addition (e.g., LC-Fining) technology. Syncrude Canada Ltd. uses the LC-Finer^{SM} hydroprocessor to reduce the carbon-to-hydrogen ratio of the atmospheric and vacuum tower residues via a combination of thermal cracking and hydrogen addition. In addition, the LC-Finer^{SM} can effectively remove sulphur and heavy metals from the oils resid (Speight and Ozum, 2001). The heavy liquid product stream from the LC-Finer^{SM} is further upgraded by carbon rejection technology (e.g., fluid coker), producing coke as a by-product, before being sent to fixed bed hydrotreaters for final nitrogen and sulphur removal to produce synthetic crude oil.

1.1.1 LC-Finer[SM] hydroprocessor

This thesis focuses on the LC-Finer[SM] hydroprocessor, shown in Figure 1.1, which is a co-current ebullated bed reactor operating at high temperatures and pressures of approximately 440°C and 11.7 MPa, respectively (McKnight et al., 2003). The unit is designed for heavy vacuum residues based on the following advantages (Rana et al., 2007): (i) liquid recirculation and fluidization result in approximately uniform temperature distribution, (ii) catalyst addition and withdrawal allow for continuous operation, and (iii) flexible operation based on catalyst selection and/or multi-stage configurations.

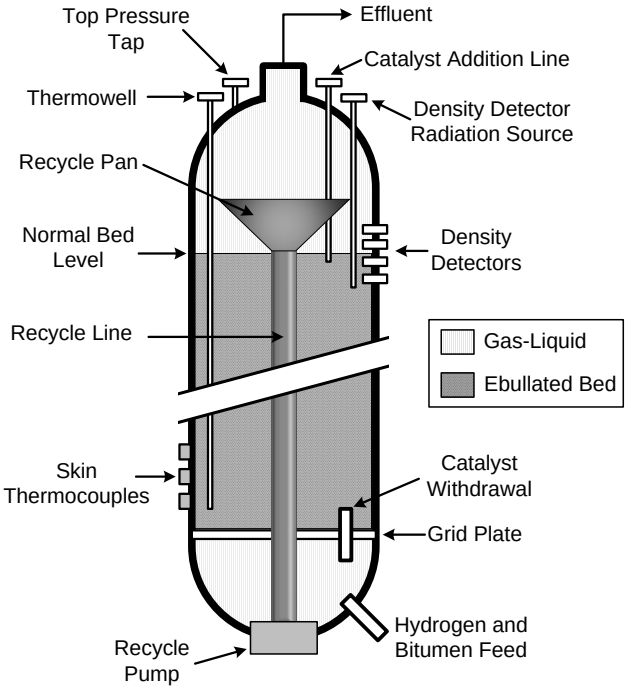

Figure 1.1: LC-Finer[SM] schematic (modified from McKnight et al., 2003).

The inlet gaseous hydrogen and liquid ATB/VTB mixture are heated separately and then fed into the plenum chamber below the grid (i.e., gas-liquid distributor plate) using a horse-shoe/shroud distributor assembly. The feed is mixed with the recycled fluid, mainly consisting of unconverted liquid and some entrained gas from the freeboard region, before flowing through the risers and bubble caps located in the grid plate. Doped alumina cylindrical catalysts are fluidized by the co-current gas and liquid flow, where liquid can be considered the continuous phase while the hydrogen and catalyst constitute the dispersed phases. Above the fluidized bed, the liquid is recirculated to the plenum chamber using a recycle pan and pump. The liquid recirculation

provides the necessary flow to fluidize the catalyst particles while also maintaining temperature uniformity throughout the reactor. Catalyst addition/withdrawal rates are varied to sustain the catalytic activity and an optimal recycle pump speed (e.g., an increase bed inventory will reduce the required pump speed to maintain the desired ebullated bed height).

1.2 Fluid dynamic studies under hydroprocessing conditions

Most research on gas-liquid-solid fluidized beds has been completed under ambient operating conditions using air, mono-component liquids (e.g., water) and spherical particle having uniform physical properties (e.g., glass beads) (Wild and Poncin, 1996). However, such conditions can significantly differ from hydroprocessors as they operate under elevated temperature and pressure, utilise non-spherical particles, and have multi-component liquids.

Global gas holdups and bubble characteristics within the range of hydroprocessing conditions have been previously investigated in slurry bubble columns (Ishibashi et al., 2001; Luo et al., 1999; Tarmy et al., 1984). Slurry bubble columns are similar to ebullated beds, however, the particles used are significantly smaller (i.e., sub-millimetre range) and are fluidized by the induced bubble wake. As a result, the liquid-solid suspension is often treated as a pseudo-homogeneous mixture. Sustained dispersed bubble flow, characterised by relatively small uniform size bubbles, at high gas holdups (e.g., greater than 25%) has been reported by Tarmy et al. (1984) and Ishibashi et al. (2001) in pilot-scale coal liquefaction slurry bubble column reactors operating at pressures up to 20 MPa and temperatures up to 450°C. It has been discussed that the high gas holdups reported were attributed to the large kinetic energy of the high pressure inlet gas and the presence of surface-active compounds in the liquid phase. Luo et al., (1999) investigated the impact of operating pressure on the bubble dynamic using Paratherm NF heat transfer fluid and pressures up to 5.62 MPa, and concluded that elevated pressure increased the bubble break-up rate, thereby reducing the maximum stable bubble size. These experiments provided relevant observations on bubble characteristics at industrially relevant operating conditions, however larger solid particles and increased liquid flow rates must be considered for an ebullated bed.

There is a limited quantity of available literature studies on ebullated beds at elevated pressure due to the liquid recirculation which increase pilot-scale equipment cost. To simulate hydrotreating/coal liquefaction fluid dynamics conditions, Fan et al. (1987) and Song et al.

(1989) performed ebullated bed experiments using air and an 0.5 wt.% aqueous t-pentanol solution in a cold flow system. The use of surface-active compounds led to bubble coalescence inhibition, yielding high gas holdups conditions. However, even though global gas holdups in the range of hydroprocessing units were observed, the use of surfactants did not reproduce commercial units' overall fluidized bed fluid dynamic due to the elevated pressure impacting local bubble behaviour. High pressure (i.e., up to 15 MPa) ebullated bed experiments were carried out by Ruiz et al. (2005, 2004) using nitrogen, glass beads, and diesel fuel. Reduced minimum liquid fluidization velocity and relative increase in gas holdup was observed but did not result in sufficiently high gas holdups in comparison to the industrial units. Pjontek et al. (2015) reported high gas holdups (i.e., greater than 40%) in ebullated bed experiments using dimensional analysis and similitude when bubble coalescence was consistently and sufficiently inhibited while operating at elevated pressure and using a 0.5 wt.% aqueous ethanol solution. The impact of increased liquid viscosity, varying superficial gas velocity and varying superficial liquid velocity were reported on global phase holdups. However, local bubble characteristics measurements at industrially relevant operating conditions were not reported in this study.

1.3 LC-Finer's optimization through fluid dynamic studies

Based on the industrial unit performance, it is believed that the LC-Finer^{SM} is limited by the reaction kinetics. As a result, its performance can be improved by investigating fluid dynamic features such as the bed and freeboard holdups, and fluidization behaviour. These parameters affect performance criteria such as pitch conversion, hydrogen utilization, distillate product yields, and energy efficiency, which are related to the environmental impact of synthetic crude oil production.

1.3.1 Bed and freeboard holdups

High gas holdups (e.g.,~ 55%) have been reported in the freeboard region of the LC-Finer^{SM} caused in part by gas recirculation via the liquid recycle line (McKnight et al., 2003). Computational fluid dynamic simulations previously suggested that the upper region of the reactor and recycle pan was not operating in a liquid-flooded regime and hence presented non-optimal conditions for gas-liquid separation. The liquid recycle pan in the freeboard region was previously redesigned where the goal was to reduce the quantity of recycled gas (McKnight et al., 2003) However, lesser than expected improvement was observed on the industrial unit. The

gas phase separation efficiency of the recycle pan is critical, as residue conversion is highly dependent on liquid residence time, where minimization of the reactor gas holdup is desired. The investigation of local bubble characteristics (e.g., bubble size distributions, bubble rise velocities, and local gas holdups) in multi-component liquids and elevated pressures can support the design, operation, and optimization of future industrial gas-liquid separation simulations and techniques.

1.3.2 Fluidization behaviour

Sufficient catalyst mixing is required to maintain catalytic activity and local temperatures throughout the ebullated bed. To maintain the reactor's catalytic activity, fresh catalyst is continuously fed to the reactor while spent (or equilibrium) catalyst is withdrawn. During demetalization and catalytic cracking of heavy oil residue, heavy metal and coke will deposit into the catalyst pores which will foul and deactivate the catalyst due to pore volume reduction. As a result, a relatively wide particle density distribution is present due to varying particle residence time within the reactor. Having a particle density distribution inside the reactor can significantly affect bed behaviour, especially the bed-freeboard interface. The catalyst bed level is monitored using gamma-ray density detectors before and after the bed-freeboard interface as previously shown in Figure 1.1. A sharp interface between the ebullated bed and freeboard regions is desired to control the bed level, where liquid and solid properties as well as local bubble flow behaviour can influence the solid disengagement zone. In addition, catalyst entrainment into the recycle pan is undesirable as it can damage the recycle pump and cause unplanned downtime. Further understanding the general fluidization behaviour (i.e., bed-freeboard interface dynamic and local solid holdups profile) would help the control of the unit, prevent catalyst carry-over into the gas-liquid separator, and maintain catalytic activity.

1.4 Research objectives

The main objective of this masters' thesis is to investigate the fluid dynamics of the ebullated bed hydroprocessor. The following provides the scope of the present work:

- Experimentally determine bubble characteristics at industrial operating conditions for the optimization and design of the recycle pan;
- Investigate the impact of a solid particle density distribution on the bed dynamic of an ebullated bed.

The effects of gas and liquid superficial velocities will be continuously evaluated throughout the experiments due to their relevance for hydroprocessors. Entrained gas from the freeboard region in the commercial unit is recycled and mixed with the feed gas and liquid below the distributor plate. Consequently, the gas recycle fraction can be essentially studied by varying the inlet gas flow rate in the experimental system as no gas is recycled with the liquid. The rotational speed of the industrial liquid recycle pump is used to control the ebullated bed height and is comparable to varying the experimental liquid superficial velocity.

2 Bubble swarm characteristics in a bubble column under high gas holdup conditions

Valois Parisien[a], Alixia Farrell[a], Dominic Pjontek[b], Craig A. McKnight[c], Jason Wiens[c], Arturo Macchi[a]

[a]*Centre for Catalysis Research and Innovation, Department of Chemical and Biological Engineering, University of Ottawa, Ottawa, Ontario, Canada, K1N 6N5*

[b] *Chemical and Biochemical Engineering Department, University of Western Ontario, London, Ontario, Canada, N6A 5B9*

[c] *Syncrude Canada Ltd., 9421-17 Avenue, Edmonton, Alberta, Canada, T6N 1H4*

Abstract

Local bubble characteristics were measured using a novel monofibre optical probe manufactured for elevated pressures and high gas holdups. The objective of this study is to test the performance of the optical probe, as well as to investigate the impact of operating conditions on bubble characteristics in a bubble column when operating under high gas holdup conditions. Experiments were conducted in a 101.6 mm diameter column operating at pressures up to 6.5 MPa. A 0.5 wt% aqueous ethanol solution was used in this study to simulate high gas holdups observed in many industrial reactors containing liquid mixtures with surface-active compounds. The probe struggled to detect all the bubbles due to significant bubble size reduction and non-rectilinear bubble rise. However, successfully detected bubbles were deemed representative of the mean bubble rise velocity as indicated by the dynamic gas disengagement technique. Global gas holdup profiles in conjunction with the drift flux analysis showed that pressure does not have a significant impact at elevated liquid flow rates as bubbles tend to follow the convective current of the liquid. Relatively narrow chord length distributions were observed, where 90% of the bubbles were 1.0 mm or less. The energy dissipated through the gas-liquid distributor plate was shown to have a significant impact on the initial bubble size generated and high gas holdups were also achieved at atmospheric pressure by varying the open-surface area of the distributor.

***This manuscript has been submitted to:** Chemical Engineering Science (CES-D-15-01734)

2.1 Introduction

Most commercial bubble columns and three-phase fluidized beds reactors operate at elevated pressures with complex multi-component liquids. However, fluid dynamic studies on multiphase systems are often conducted with water at atmospheric condition. Fan (1999) previously discussed that increasing pressure leads to enhanced bubble breakup due to the Kevin–Helmholtz instability and internal circulation of the gas, reducing the mean bubble size and generating narrower size distributions. As a result, single bubble rise velocities also decrease with pressure. It is generally accepted that an elevation in pressure delays flow regime transition and further increases gas holdup (Fan et al., 1999; Kemoun et al., 2001; Krishna et al., 1991; Wilkinson and Dierendonck, 1990). However, no up-to-date accurate prediction tool for gas holdups at elevated pressure has been developed due to the sparsity of experimental results (Leonard et al., 2015). In comparison to single bubble behaviour, bubble swarm dynamics is rather difficult to predict as swarm drag corrections are directly related to the gas holdup.

The foaming tendency of multi-component liquids significantly increase gas holdups due to surface-active compounds inhibiting bubble coalescence and to bubble size reduction (Camarasa et al., 1999; Jamialahmadi and Müller-Steinhagen, 1992; Keitel and Onken, 1982; Kelkar et al., 1983; Macchi, 2002; Rollbusch et al., 2015). Single bubble behaviour in contaminated systems has been studied by various investigators. Surface-active compounds tend to accumulate at the gas-liquid interface inducing a surface tension gradient, due to the adsorbed contaminants being swept to the bubble rear as it rises through a liquid, which opposes tangential shear stresses (Levich and Spalding, 1962). Moreover, small bubbles generated in the system behave as rigid spheres (Shah et al., 1985) which increases drag on the bubbles and reduces the rise velocity (Clift et al., 2005; Levich and Spalding, 1962). In addition to swarm effects due to gas holdups; the impact of multi-component liquids on bubble rise velocity is still unclear.

The investigation of local bubble characteristics (e.g., bubble size distributions, bubble rise velocities, and local gas holdups) in multi-component liquids and elevated pressures can support the design, operation, and optimization of industrial bubble columns and ebullated bed reactors. The unit of interest for this study is the LC-Finer^{SM} resid hydroprocessor which operates at pressures and temperatures of approximately 11.7 MPa and 440°C, respectively (McKnight et al., 2003). High gas holdups have been reported for such hydroprocessors and are

thought to be caused in part by gas recirculation via the liquid recycle line. The liquid recycle pan in the freeboard region was previously redesigned with the aid of computational fluid dynamic (CFD) simulations, where the goal was to reduce the quantity of recycled gas (McKnight et al., 2003).As computational times for CFD modeling are continually reduced and measurement techniques are improved, local bubble properties measured under high gas holdup conditions can be used to improve gas-liquid separation simulations and techniques.

Bubble properties in gas-liquid and gas-liquid-solid systems have been previously investigated using various measurement devices (Boyer et al., 2002). As discussed by Pjontek et al., (2014b) and Boyer et al., (2002), most measurement techniques fail to accurately measure the local bubble characteristics of interest at high gas holdup fractions due to insufficient response time and/or physical limitation of the measurement device (e.g., bubble sizes below detection limits). Following the work of Pjontek et al., (2014b), a prototype monofiber optical probe combining both 1C (conical) and 3C (conical-cylinder-conical) geometrical characteristics (Mena et al., 2008) has been manufactured for elevated pressures and high gas holdup conditions, details of which are in section 2.2.2.1

The objective of this study is to test the performance of the novel monofibre optical probe configuration for bubble characterization, as well as investigate the impact of operating conditions on bubble characteristics in a bubble column when operating under high gas holdup conditions relevant to the freeboard of the LC-Finer^{SM}. The optical probe performance was assessed by comparing global measurements to integrated local gas holdups in water and an aqueous ethanol solution while the measured average bubble swarm rise velocities were compared to estimates based on the dynamic gas disengagement technique. The effect of operating conditions on local bubble rise velocities and bubble chord length distributions is presented and the impact of energy dissipation at the gas-liquid distributor to achieve high gas holdups is discussed.

2.2 Materials and methods

2.2.1 Experimental setup

Experiments were carried out in a stainless steel column with an inner diameter of 101.6 mm and height of 1.8 m capable of reaching pressures up to 10 MPa. The system was pressurized using industrial grade nitrogen cylinders. A centrifugal pump drives the liquid from the storage tank to the base of the column and a magnetic flow meter (Rosemount model: 8732CT12N0) measures the liquid flow rate. Gas was circulated via a single stage reciprocating compressor, where fluctuations in the gas flow are reduced by upstream and downstream gas dampeners. A differential pressure transducer and orifice plates of varying size, depending on the operating pressure, were used to measure the gas flow rate. Gas was sparged in the plenum chamber of the column (i.e., below the distributor plate) via a sintered pipe with 10 μm diameter pores. The gas–liquid mixture then flowed through a perforated distributor plate with 23 holes of 3.175 mm diameter. Three glass viewing windows are located above the distributor plate. Global phase holdups were determined using a differential pressure transmitter (Rosemount, model: 1151DP3S22C6Q4). The optical probe was inserted into the column at a height of 1045 mm above the distributor to minimize the impact of entrance effects. At high gas holdup conditions, bubble characteristics in the freeboard of the ebullated bed were found to be similar to those of a bubble column operated at the same fluid superficial velocities (McKnight et al., 2003; Pjontek et al., 2014). Bubble column experiments thus prevent the possibility of damaging the probe from particles entrainment into the freeboard. A schematic of the experimental system and additional details can be found in Pjontek et al., (2014b). Operating conditions and phase physical properties for this study, presented in Table 2.1 were chosen to provide high gas holdups relevant to ebullated bed hydroprocessors.

Table 2.1: Experimental operating conditions and fluid properties.

Parameter	Symbol	Range	Units
Superficial liquid velocity	U_L	0 – 107	mm/s
Superficial gas velocity	U_G	0 – 105	mm/s
Pressure	P	0.1 – 6.5	MPa
Temperature	T	22 – 24	°C
Liquid density	ρ_L	997	kg/m^3
Liquid viscosity	μ_L	0.001	Pa·s
Gas density	ρ_G	1.5 – 74	kg/m^3

A 0.5 wt% aqueous ethanol solution was used to inhibit bubble coalescence and increase gas holdups. Ethanol was selected as a surfactant as it produces an effervescent foam at the free surface (Dargar and Macchi, 2006), which is required to prevent gas recirculation throughout the experimental system (Pjontek et al., 2014). The combined effects of elevated pressures and surface-active compounds are relevant to industrial bubble columns and gas-liquid-solid fluidized beds, where gas holdups are considerably greater than in atmospheric air-water systems (McKnight et al., 2003). Tap water was first used to validate global measurements obtained by the optical probe and dynamic gas disengagement (refer to Section 2.2.2.3).

2.2.2 Measurement techniques

During the experiments, local bubble properties were measured using a monofibre optical probe, global phase holdups were determined using the differential pressure transducer, and gas holdup structures and average bubble rise velocities were obtained using the dynamic gas disengagement technique. To compare with the optical probe, the dynamic gas disengagement technique was extended to continuous liquid flow operation by measuring the dynamic pressure drop during the disengagement process. Once the system reached steady state, all measurements were taken to ensure proper comparison between global and local values.

2.2.2.1 Monofibre optical probe

A prototype monofiber optical probe was manufactured by A2 Photonic Sensors for high pressure and high gas holdup conditions. Optical probes can distinguish between phases (e.g., gas-liquid, liquid-liquid, and gas-liquid-solid) due to differences in refractive index. A monochromatic light (i.e., laser) is transmitted from the optical fiber to the probe tip which is then reflected and/or refracted at varying intensities depending on the probe tip geometry and

phases involved. When the tip is immersed in liquid, the light is scattered and does not reflect back into the emitter/receiver device. Since the gas has a lower refractive index compared to the liquid, light is reflected at a greater intensity when the tip is submerged in gas. The resulting electrical signal clearly distinguishes between the gas and liquid phases, allowing local bubble properties to be measured from the total time immersed in the different phases, and individual signals' duration and rise time. Further details can be found in Mena et al., (2008).

The probe geometry resembles a 3C probe but the sensing tip length is reduced below the typical range of a 1C probe. This design combines the accuracy and precision of a 3C probe and the higher detection limit of the 1C probe configuration for smaller bubbles (Cartellier and Barrau, 1998). The shorter sensing length ($L_s \approx 30$ μm for the studied probe) is better adapted for bubbles in the range of 1 mm and lower in diameter. Monofibre optical probes can simultaneously measure local gas holdups, bubble rise velocities, and chord lengths by knowing the length of the sensing tip (L_s). This probe characteristic must be determined through calibration prior to experiments, where an example of a calibration curve is provided by Mena et al. (2008). The probe signal is measured via an optoelectronic module which emits a laser beam to the probe tip and converts the reflected optical signal into a digital signal.

Local gas holdups ($\varepsilon_G(r)$) are calculated as the ratio of the cumulated bubble residence times ($t_{b,i}$) on the probe tip over the total measurement time (t_T).

$$\varepsilon_G(r) = \frac{\sum_i t_{b,i}}{t_T} \tag{2.1}$$

Individual bubble rise velocities ($u_{b,i}$) are estimated based on the probe sensing length and the signal rise time ($t_{R,i}$), which is the time observed between selected lower and upper thresholds based on the gas and liquid voltage difference. Lower and upper thresholds of 10% and 90% were used for these experiments based on recommendations from the manufacturer.

$$u_{b,i} = \frac{L_s}{t_{R,i}} \tag{2.2}$$

Knowing the rise velocity and residence time, the individual bubble chord length ($c_{b,i}$) can be determined using the following relation:

$$c_{b,i} = u_{b,i} t_{b,i} \tag{2.3}$$

It should be noted that rise velocities and chord lengths in this study are only provided for fully detected bubbles (i.e., when the signal exceeds the upper threshold). However, bubble residence times used for local holdups take into account all signals which exceed the liquid voltage, while also accounting for signal noise.

The digital signal obtained by the optoelectronic module was analyzed by the SO6 software provided by A2 Photonic Sensors. Rise times and residence times were recorded for each bubble. Signals that do not reach the upper threshold are distinguished from fully detected bubbles. This may occur if the bubble is small relative to the probe sensing length or if the bubble is pierced off-centre. Data acquisition was dependent on the number of bubbles measured or a set time limit. For all results, data was gathered for at least 120 seconds and with a minimum of 5000 bubbles at a frequency of 200 Hz.

2.2.2.2 Global gas holdups

Global gas holdups were determined by measuring the dynamic pressure drop. Neglecting frictional drag on the wall and accelerations of the phases in the vertical direction, the global gas holdups (ε_G) were calculated using the measured axial dynamic pressure profile.

$$\varepsilon_G = \frac{\Delta P / \Delta z}{g(\rho_L - \rho_G)} \tag{2.4}$$

2.2.2.3 Dynamic Gas Disengagement

The gas holdup structure was investigated using the dynamic gas disengagement technique (DGD). The DGD technique, originally proposed by Sriram and Mann (1977), consists of shutting the gas feed to the column and tracking the bubbling height during the disengagement process in a batch liquid system. The technique was restricted by constant visual observation of the liquid level inside the column, limiting the use of an opaque system. To overcome this limitation, Daly et al., (1992) extended the technique by measuring pressure transducer signals to estimate the rate of the liquid level drop as well as reducing uncertainties related to large bubbles disengaging. The rate of liquid height or pressure drop at any given time is related to the average

bubble population leaving the system at that instant, enabling the estimation of the holdup structure and bubble rise velocities prior to gas flow interruption.

In this study, the DGD technique was extended from batch to continuous liquid flow operation to estimate the impact of liquid flow on gas holdup and swarm rise velocity by measuring the dynamic pressure drop across the reference and highest available pressure port of the column during the disengagement process. Pressure drop caused by friction at the wall was measured and was deemed a negligible contribution to the dynamic pressure (less than 0.3 %) due to the gas disengagement. The analysis of DGD profiles relies on the following assumptions to estimate the average rise velocity of each bubble class: (1) no bubble-bubble interaction (i.e., coalescence or breakup) during disengagement, (2) bubble dispersion is axially homogeneous prior to gas interruption, (3) all bubbles disengage independently (i.e., constant rate disengagement process), (4) axial liquid deceleration caused by bubble disengagement is negligible. This last assumption was verified at the highest liquid velocity tested and was deemed negligible with a maximum gas holdup contribution of 0.14 vol.%. A material balance on the gas phase leads to the following expression:

$$-\frac{d\varepsilon_{G,j}}{dt}\Delta z = \sum_{i=j}^{N} u_{b,i}\varepsilon_{G,i} \tag{2.5}$$

The gas holdup of each bubble class is determined by extending the disengagement rate of each bubble class to t = 0 (i.e., time of gas shut-off). The average bubble swarm rise velocity of the population is determined using the gas holdup and slope of each class. The disengagement process was recorded for a period of 30 seconds at a sampling frequency of 40 Hz.

2.3 Techniques validation at high gas holdups

2.3.1 Gas holdup

The optical probe measurements were first validated by comparing the integrated radial gas holdup profiles to the global gas holdups measured using the dynamic pressure drop.

$$\varepsilon_G = \frac{1}{\pi R^2}\int_0^R \varepsilon_G(r)2\pi r\,dr \tag{2.6}$$

Measurements were taken in both water and the 0.5 wt% aqueous ethanol solution. All experimental conditions investigated in this study using the ethanol solution are presented in

Figure 2.1, whereas a subset of conditions was studied using tap water. The results show that the integrated local measurements in the water system were within ± 10% of the global measurements with an average relative deviation of 4.7%. Local measurements in the aqueous ethanol solution under predicted the global values with an average relative deviation of 59.6%. Similar performance has been reported by Pjontek et al., (2014b) using a 1C monofiber optical probe, where a combination of the optical probe's physical limitations and a change in bubble flow direction are believed to have inhibited the probe measurements.

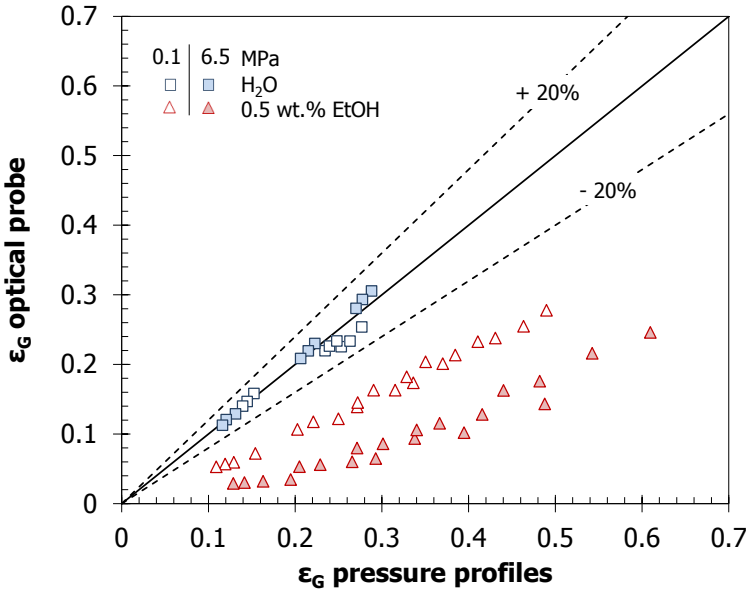

Figure 2.1: Comparison of global and integrated local gas holdups.

The percentage of fully detected bubbles (i.e., when the bubble signal reached the upper voltage threshold) at high pressure was in the range of 50% to 65% for the prototype 1C-3C probe, in comparison to 20% to 40% with the 1C optical probe (Pjontek et al., 2014). This demonstrates that the prototype optical probe geometry is better suited to detect smaller bubbles in comparison to the previous configuration. The underestimation of the gas holdup in the aqueous ethanol solution at low and high pressure can be caused by two synergistic phenomena. The added ethanol and increased pressure significantly reduced the bubble size population below 1 mm (further discussed in Section 2.5.2) thus possibly increasing a portion of the bubble size population below the lower detection limit of the probe. This bubble size reduction likely increases the drifting effect (i.e., altered bubble trajectory prior to the probe tip piercing) and thus resulting in lower local gas holdups due to preferential detection/piercing of larger bubbles.

Bubbles were visually observed through the windows to follow the convective currents of the liquid stream, where a significant portion of bubbles was not rising rectilinearly inside the column. Since the optical probe can only measure bubbles rising upward, the underestimated gas holdups are in agreement with the visual observations.

2.3.2 Average bubble rise velocity

The optical probe performance was also examined by comparing the bubble swarm rise velocity measurements to the DGD estimates. The local rise velocity was approximated by the arithmetic average of the entire bubble population at that location. Rise velocity measurements from the optical probe were then integrated over the column cross-sectional area, equation (2.7), whereas the weighted average velocities over all bubble class measured was taken for the DGD, equation (2.8).

$$U_b = \frac{1}{\pi R^2 N_b} \int_0^R u_b n_b 2\pi r dr \tag{2.7}$$

$$U_b = \frac{1}{\varepsilon_G} \sum_i^N \overline{u}_{b,i} \varepsilon_{G,i} \tag{2.8}$$

Figure 2.2 demonstrates that the integrated local measurements in water and the 0.5 wt% aqueous ethanol were generally within ± 30% of the global measurements, with an average relative deviation of 7.7% and 16.6%, respectively. It should be noted that results for superficial gas velocity smaller or equal to 52.5 mm/s are presented in Figure 2.2, as there is a higher confidence in the DGD technique at these conditions. For greater velocities, the independent bubble disengagement assumption is no longer applicable due to bubble-bubble interactions (Lee et al., 1999).

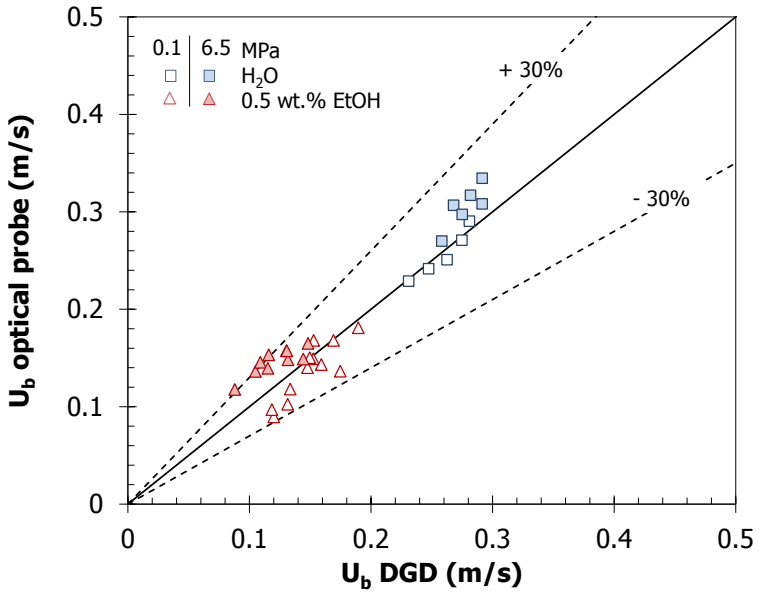

Figure 2.2: Comparison of cross-sectional average bubble rise velocities.

Results indicate that even if the probe does not fully detect each bubble hitting the probe tip, those that are fully detected are representative of the mean rise velocity measured by the DGD. This suggests that the size distribution is relatively narrow and/or that the slip velocity is small, as demonstrated with the linear DGD profiles in Figure 2.3a. Overestimation of the average bubble rise velocity at elevated pressure was observed and can be associated again with the lower detection limit of the probe and bubble size reduction thus preferentially piercing larger bubbles having greater rise velocities. However, due to the close agreement between both measurement methods (average relative deviation of 7.7% and 16.6% as mentioned in discussion relative to Figure 2.2), there is confidence in the individual optical probe measurements. If a relatively wide bubble size distribution was present in the system and the slip velocity was significant, multiple disengagement slopes would be observed, as shown in Figure 2.3b for a 152 mm inner diameter column system having a distributor with a greater open-surface area and having gas injected at distributor level (presented in Section 2.6).

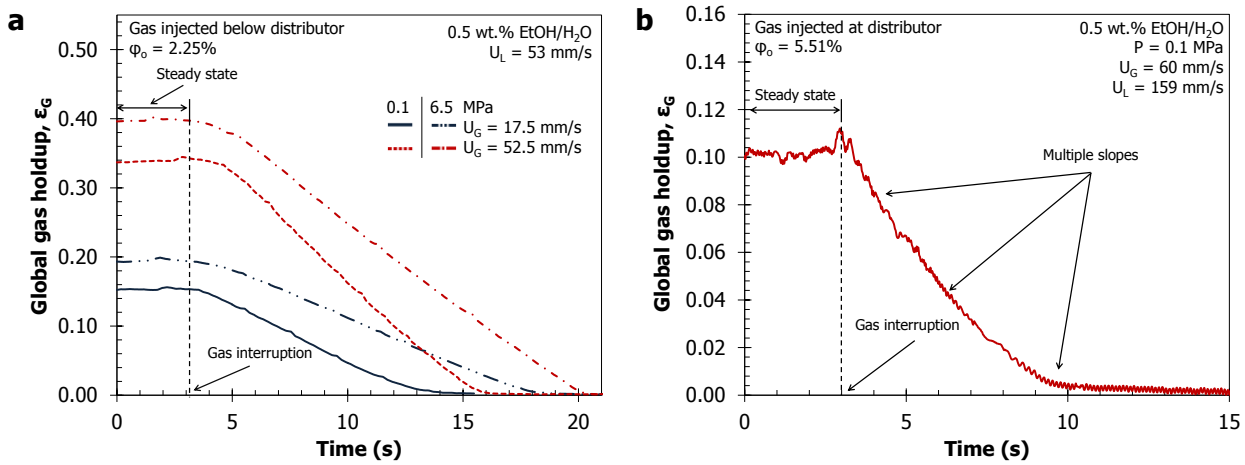

Figure 2.3: Dynamic gas disengagement profiles for different gas-liquid distributor designs.

2.3.3 Average bubble size

The average bubble size of the population was also estimated based on the swarm velocity determined with the DGD. This was only performed with the aqueous ethanol solution since the observed bubbles were spherical ($Eo < 1$) and the size distribution is likely to be narrower. To isolate the bubble swarm rise velocity from the increased velocity due to liquid flow, the mean interstitial liquid velocity was subtracted from rise velocity measured. The Tomiyama (1998) single bubble drag model for fully contaminated systems was chosen due to its large range of applicability. The Lockett and Kirkpatrick (1975) swarm drag correction was selected as it was developed using global gas holdups measurements up to 66%.

$$C_{D,\infty} = \max\left\{\frac{24}{Re_b}\left(1 + 0.15Re_b^{0.687}\right), \frac{8}{3}\frac{Eo}{Eo + 4}\right\} \tag{2.9}$$

$$\frac{C_{D,swarm}}{C_{D,\infty}\left(1 - \varepsilon_G\right)} = \left[\left(1 - \varepsilon_G\right)^{1.39}\left(1 + 2.55\varepsilon_G^{3}\right)\right]^{-2} \tag{2.10}$$

$$U_{slip} = U_b - \frac{U_L}{1 - \varepsilon_G} = \sqrt{\frac{4}{3}\frac{gd_b}{C_{D,swarm}}\left(\frac{\rho_L - \rho_G}{\rho_L}\right)} \tag{2.11}$$

As discussed by Simonnet et al., (2007) and Roghair et al., (2011), multiple swarm drag corrections are proposed in the literature where most models are limited to low gas fractions ($\varepsilon_G < 0.10$) and diverge significantly at high gas holdup ($0.10 < \varepsilon_G < 0.50$). Therefore, careful attention must be made to choose the most appropriate drag model and interpret the validity of the results. Estimated bubble sizes using the previous correlations range from 0.16 mm to 0.56

mm in diameter for both high and low pressure conditions. To convert the chord lengths measured with the optical probe to actual bubble sizes, a 1.5 scaling factor has been used by various investigators (Esmaeili et al., 2015; Shah et al., 1985; Simonnet et al., 2007) which is in relatively good agreement with the DGD results (further discussed in Section 2.5.2). Based on the bubble sizes and rise velocities measured from the optical probe, bubbles were generally between the Stokes and intermediate flow regimes ($1 < Re_b < 35$), where viscous forces are still important.

2.4 Global measurements

2.4.1 Gas holdup

Global gas holdups obtained with the aqueous ethanol solution, presented in Figure 2.4, were first investigated to observe the impact of operating conditions and to identify the bubble flow regimes. Batch liquid operation was not investigated in this study as the entire system would evolve to a froth/foam at relatively low gas velocities, particularly when the pressure is increased above 0.1 MPa. Error bars were omitted in Figure 2.4 as the coefficient of variation of replicates was less than 1%.

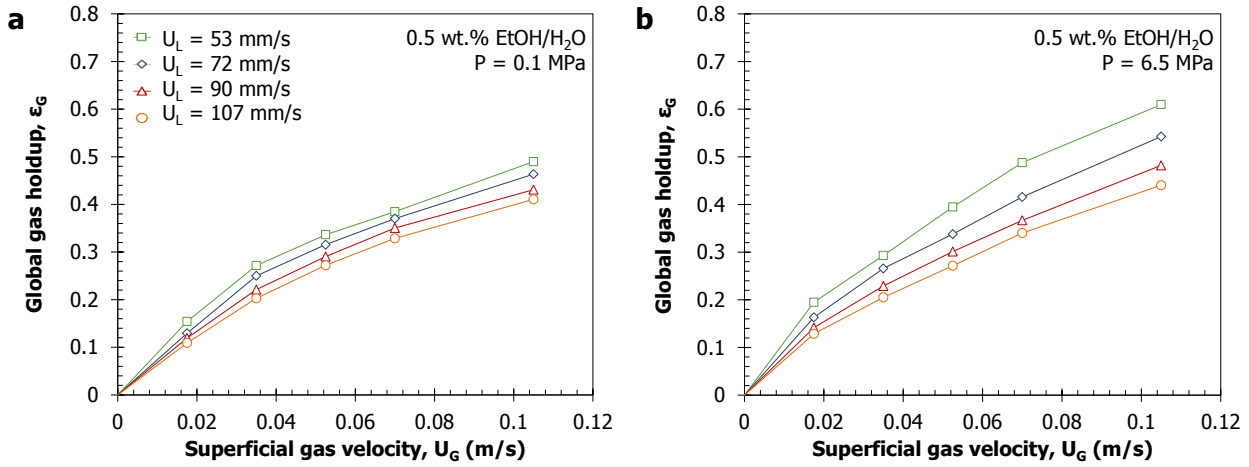

Figure 2.4: Global gas holdups as a function of superficial gas and liquid velocities.

The impact of pressure on global gas holdups was more apparent at lower liquid velocities (U_L < 90 mm/s) where the lower shear stress at the distributor formed larger bubbles that were then subject to greater bubble breakup (Krishna et al., 1991; Pjontek et al., 2014; Rudkevitch and Macchi, 2008). Higher operating pressures enhance bubble breakup and lower

the maximum stable bubble size due to a combination of the Kevin-Helmholtz instability between two fluids (Wilkinson and Dierendonck, 1990) and the internal circulation of the gas model (Levich and Spalding, 1962). The Kevin-Helmholtz instability model is based on a critical wavelength, which is a function of the gas density, where disturbances exceeding that critical value render the bubble interface unstable, resulting in bubble breakup. The internal circulation model, however, predicts that a centrifugal force pointing outward is induced which counter-balances the surface force. As pressure increases, the centrifugal force becomes larger than the surface force, which stretches the bubble interface and breaks the bubble. Increased pressure had a minor impact on global gas holdups at liquid velocities greater than 90 mm/s. It is thought that at high gas holdups and fine dispersions, the drag forces on bubbles are more important than buoyant forces, thus resulting in bubbles being entrained with the liquid streamlines (Kelkar et al., 1983). Therefore, even though the bubble size is reduced due to pressure, the resulting impact on gas holdups is minor at such conditions.

2.4.2 Flow regime transition

From the global gas holdup trends, it is difficult to discern the bubble flow regime. The transition from dispersed/homogenous to coalesced/heterogeneous bubble flow is not sharp as presented by other investigators (Krishna et al., 1991; Letzel et al., 1997). The drift flux (j_{GL}), defined as the gas phase velocity relative to a surface moving at the same average velocity of the gas-liquid flow system (Wallis, 1969), was used to investigate flow regime transition. The drift flux can be estimated using the slip velocity of the gas obtained via the global gas holdups and the superficial gas and liquid velocities.

$$j_{GL} = \varepsilon_G \varepsilon_L \left(\frac{U_G}{\varepsilon_G} - \frac{U_L}{1 - \varepsilon_G} \right) \tag{2.12}$$

The transition from dispersed to coalesced bubble flow regimes can be estimated by plotting the drift flux as a function of global gas holdup (Wallis, 1969). In dispersed bubble flow, the drift flux increases linearly as a function of the gas holdup. As larger bubbles are generated in coalesced flow, the drift flux rises markedly faster. Provided that enough data is gathered, the intercept between the previous slopes is the flow regime transition point. Drift flux results for the operating conditions from Figure 2.4 are presented in Figure 2.5.

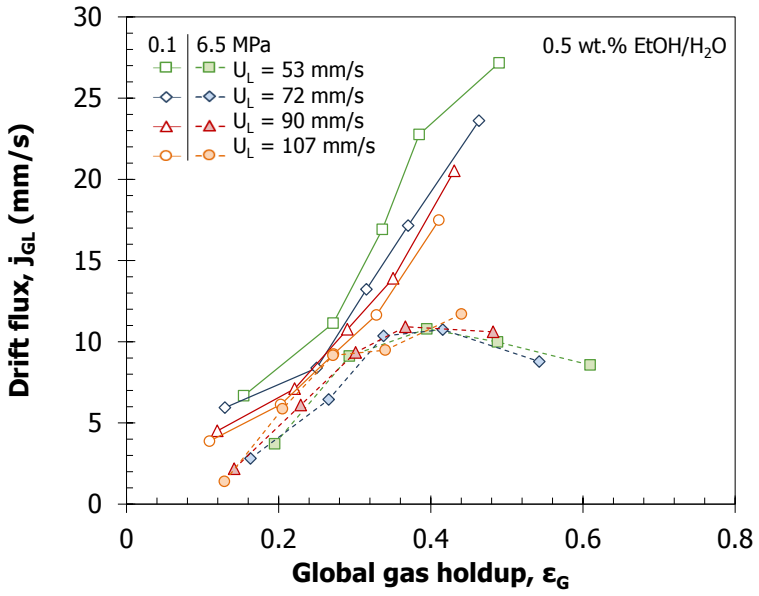

Figure 2.5: Impact of pressure on bubble flow regime transition.

At 6.5 MPa, the drift flux has a decreasing trend at higher gas holdups. This has been observed previously by Lockett and Kirkpatrick (1975) when operating counter-currently with liquid velocities equal to the rise velocity of the bubble swarm. The authors proposed that as the gas flow rate initially increases, the gas holdups and drift velocity increase due to the buoyancy of the bubbles. At the transition point (i.e., maximum drift velocity) the buoyancy force is equal to the drag force. Further increasing the gas holdups results in swarm drag becoming greater than buoyancy due to hindering effects from the increased swarm population resulting in a downward drift velocity. The elevated pressure results presented in this study indicates that bubbles do not readily coalesce for the studied co-current operation after being sheared at the distributor.

2.5 Local measurements

2.5.1 Swarm bubble rise velocity

Local average rise velocity profiles, presented in Figure 2.6, demonstrate varying behaviour depending on the operating conditions. Measurements were not performed at r/R = - 0.9 because the optical probe's length inside the column was not sufficient to reach that position. Error bars were omitted in Figure 2.6 and Figure 2.7 as the coefficient of variation of replicates was less then 5%. Flat profiles were obtained at the lowest superficial gas velocity of 17.5 mm/s (Figure 2.6a), as anticipated for well dispersed bubble flow. Higher gas flow rates resulted in greater profile curvature with a maximum at the center of the column (r/R = 0). The bubble rise

velocities measured by the probe represent the actual velocity of bubbles inside the column which takes into account the increased velocity caused by the liquid flow. Curvature in the local liquid velocity profile due to the no-slip condition at the column wall would thus increase the bubble swarm velocity at the center of the column. The liquid axial dispersion coefficient is representative of the local liquid velocity profile inside the column. Kelkar et al. (1983) showed that the dispersion coefficient in aqueous alcohol solutions vary significantly in comparison to pure systems. They demonstrated that backmixing is negligible at low gas velocities, then increases linearly with superficial gas velocity until heterogeneous bubble flow is obtained. This observation can partially explain the flat profile observed for a superficial gas velocity of 17.5 mm/s and the curved profile at 52.5 mm/s. In addition, visual observation at the column wall showed a net upward bubble flow at lower gas flow rates, whereas superficial gas velocities above 50 mm/s showed significant backmixing.

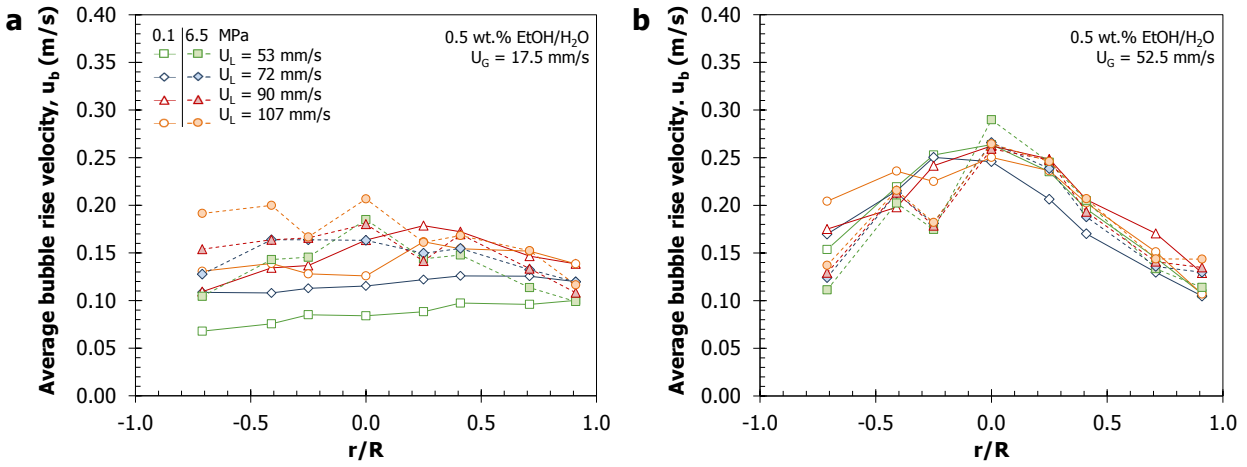

Figure 2.6: Radial average bubble rise velocity profiles at varying superficial liquid velocity and pressure.

2.5.2 Bubble chord length

Volume-average bubble chord length radial profiles, presented in Figure 2.7, are relatively flat for the investigated operating conditions. This suggests that the entire bubble population is well distributed across the column diameter. Similar results have been reported by Chen et al., (2003) in large diameter columns (i.e., inner diameter of 200, 400, and 800 mm) using a monofiber optical probe employing laser Doppler technique. Bubbles size decreased with increasing pressure, in agreement with previous studies (Fan et al., 1999; Idogawa et al., 1985;

Jin et al., 2004; Lin et al., 1998; Pjontek et al., 2014; Schäfer et al., 2002; Wilkinson and Dierendonck, 1990).

$$c_{b,vol} = \sqrt[3]{\frac{1}{N_b}\sum_{i=1}^{N_b} n_{b,i} c_{b,i}^{3}} \tag{2.13}$$

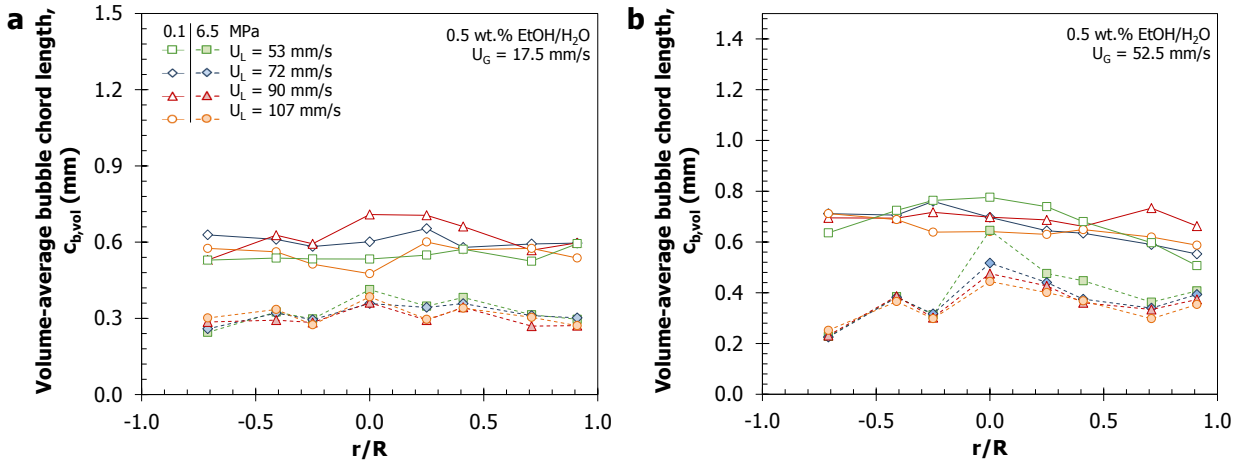

Figure 2.7: Radial volume-average bubble chord length profiles at varying superficial liquid velocity and pressure.

Bubble chord length distributions, presented in Figure. 2.8, demonstrate the impact of gas flow rate and pressure on the bubble population. The bubble population follows a log-normal distribution. It is observed that for all operating conditions investigated, approximately 50% and 90% of the bubble population is respectively below a chord length of 0.5 mm and 1.0 mm.

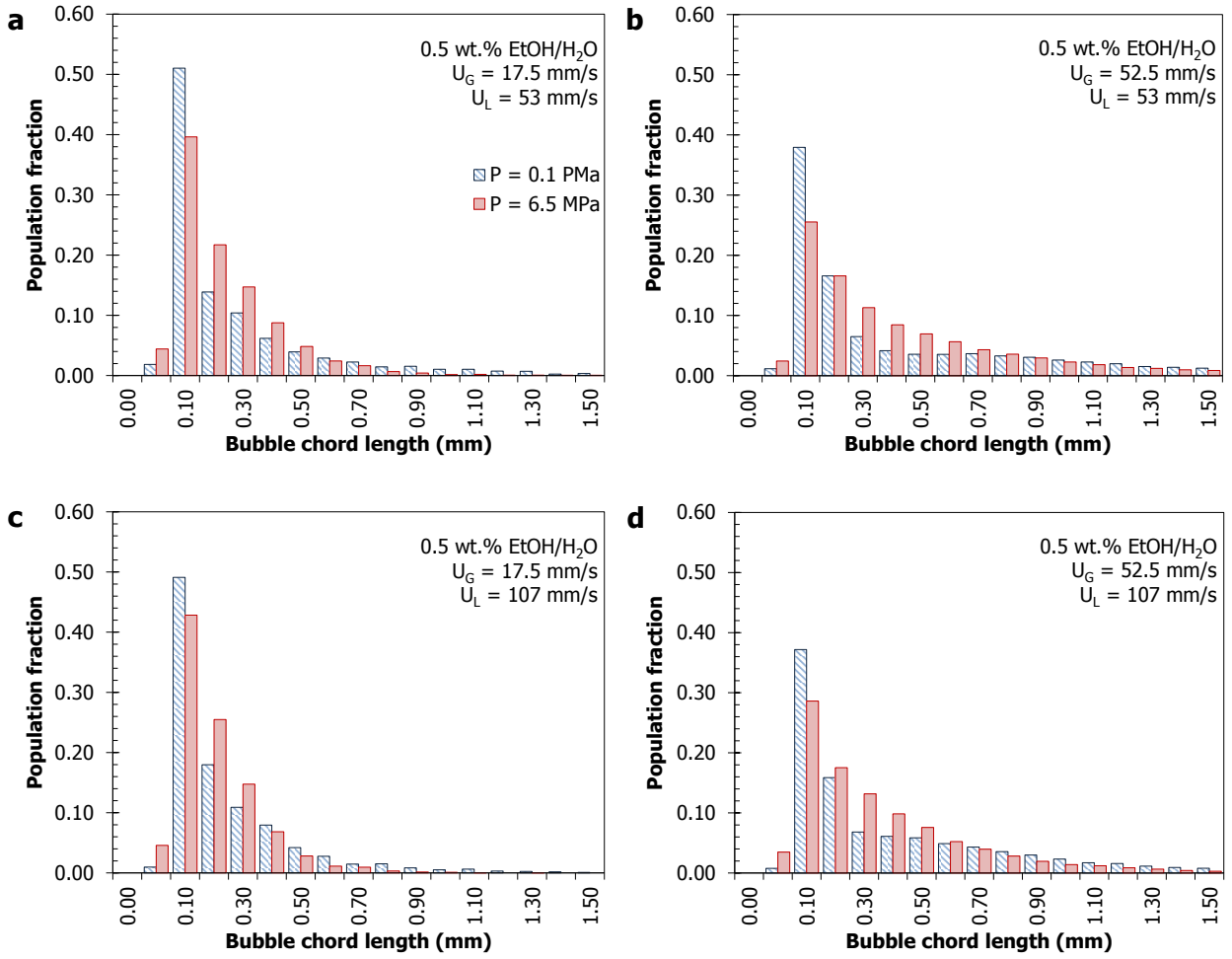

Figure. 2.8: Effect of superficial gas and liquid velocity and pressure on bubble chord length number distributions (r/R = 0).

The impact of superficial gas velocity and pressure on the integrated local volume-average bubble chord length (see equation (2.14)) is presented in Figure 2.9. The gas flow rate has a limited impact on the average chord length for the studied conditions. This trend was also reported by Idogawa et al., (1985) and Soong et al., (1997) in the dispersed bubble flow regime. It is thought that bubbles are not significantly affected by gas flow rate due to the combination of two effects. First, the shearing through the perforated plate promotes fine bubbles generation, and second the surfactant molecules and high pressure prevent bubbles to coalesce. This illustrates the importance of the initial bubble size generated in contaminated systems (Schäfer et al., 2002).

$$C_{b,vol} = \frac{1}{\pi R^2 N_b} \int_0^R c_{b,vol} n_b 2\pi r dr \qquad (2.14)$$

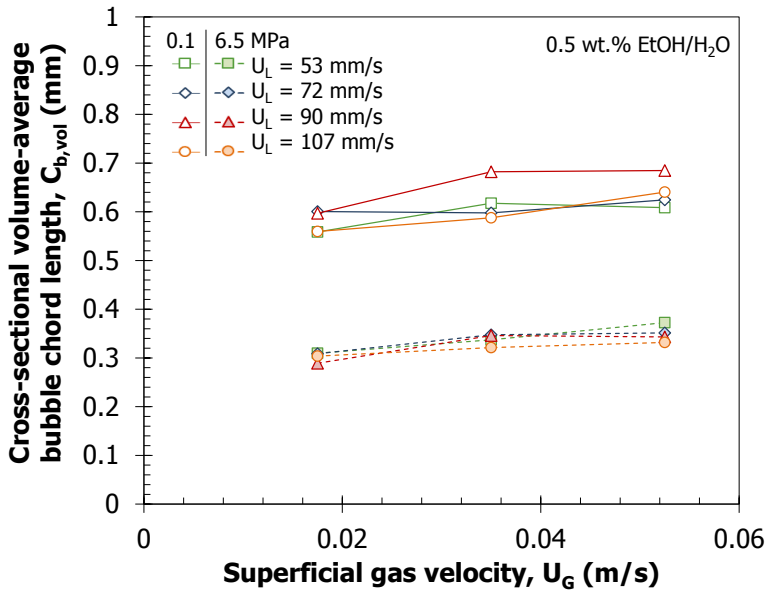

Figure 2.9: Impact of superficial gas velocity on cross-sectional volume-average bubble chord length at varying superficial liquid velocity and pressure.

After being sheared though the distributor plate to a dispersion of fine bubble, the enhanced bubble breakup due to pressure further reduces the average chord length for the investigated operating conditions. The impact of liquid flow rate on the measured average chord length seems minor in comparison to pressure.

2.6 Importance of gas-liquid distribution on high gas holdups

A complementary study on the impact of the gas-liquid distribution method on high gas holdup generation was carried out due to the importance of the initial bubble size on the resulting equilibrium bubble size, and ultimately gas-liquid separation efficiency at the top of the LC-Finer^{SM}. Experiments were initially performed in a separate co-current 152.4 mm inner diameter column operating at atmospheric pressure (referred as system "B", whereas the high pressure system is referred as system "A"). The gas and liquid were introduced separately, but at the same level. The liquid distributor is a perforated plate with 80 holes of 4.0 mm diameter, while the gas is introduced via 26 holes of 0.8 mm diameter. Tap water and a 0.5 wt.% aqueous ethanol solution were used as a bubble coalescing and coalescence inhibiting liquid, respectively. Additional details on the system can be found in Pjontek et al., (2011). Global gas holdups for both systems are compared in Figure 2.10. Significant disagreement between both experimental systems was observed for identical operating conditions. Relatively large bubbles (d_b > 3 mm)

were visually observed inside system B for both water and ethanol solution. The larger bubbles induced a vortical-spiral motion in the center region of the column, which differed from the observations made in system A.

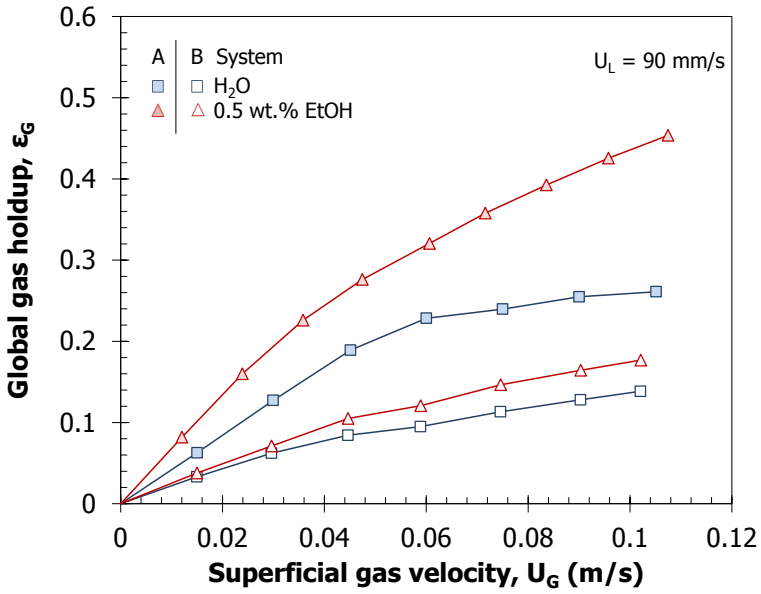

Figure 2.10: Impact of gas-liquid distribution method on global gas holdups.

A sintered pipe was installed below the liquid distributor plate of system B so that the gas-liquid mixture flows through the plate together, similar to system A. The use of porous distributor has been investigated by numerous investigators (Akita and Yoshida, 1974; Anastasiou et al., 2010; Camarasa et al., 1999; Kazakis et al., 2008) and significant increases in gas holdup were achieved. However, results demonstrate that the sintered pipe had no significant impact in water due to its coalescing nature. This discrepancy between both experimental systems is attributed to the difference in distributor plate design, specifically in terms of the energy dissipation. As discussed by Gadallah and Siddiqui, (2015), the hole diameter and plate open surface-area can significantly increase global gas holdups due to bubble breakup from flow contraction. Hinze (1955) identified the forces describing deformation and breakup of bubbles under turbulent flow conditions and showed that the maximum stable bubble size decreases as the energy dissipation increases due to more energetic eddy formation in the continuous phase.

The open surface-area (i.e., number of holes) of system B was reduced to increase the energy dissipated (i.e., pressure drop) through the distributor plate. The number of holes was estimated to obtain an equal orifice velocity and hence, energy dissipation to system A. The

global gas holdups comparison presented in Figure 2.11 shows the impact of energy dissipation through an orifice to reduce bubble size and achieve high gas holdups. This demonstrates the importance of minimizing the energy dissipation through the distributor plate to generate larger bubbles, especially at elevated pressure and in the presence of surface-active compounds as bubbles will not readily coalesce after being sheared to a fine dispersion.

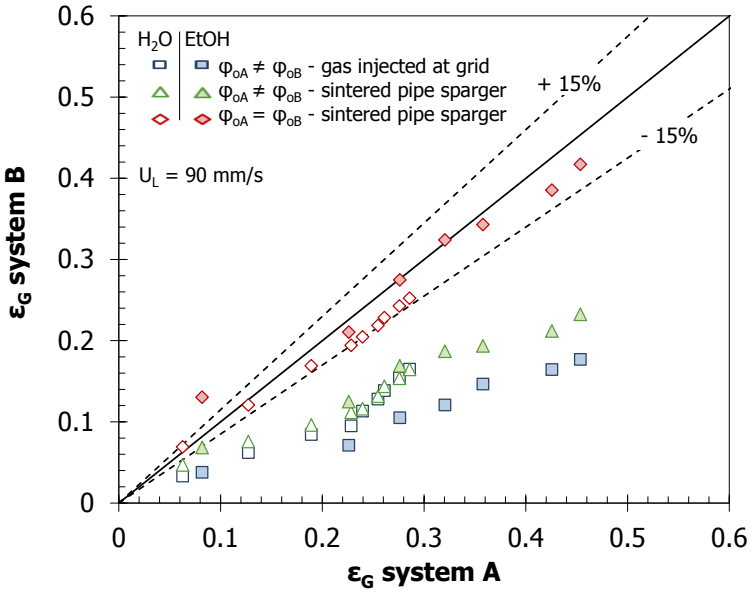

Figure 2.11: Gas holdup comparison for varying distributor energy dissipation rates

2.7 Conclusions

Bubble characteristics at high gas holdup conditions were measured using a custom-made monofibre optical probe. The probe measurements were validated using the dynamic pressure drop for global gas holdup measurements and the dynamic gas disengagement technique for the average swarm rise velocities. Based on integrated local gas holdup, the optical probe struggled to fully detect all the bubble population due to the reduced bubble size induced by elevated pressure and surfactant addition, and also because of the non-rectilinear rise of bubbles. However, the swarm rise velocity and bubble size measurements using the optical probe demonstrated good agreement with the DGD results, providing confidence in the optical probe measurements based on fully detected bubbles.

Elevated pressure and surfactant addition promoted high gas holdup conditions by reducing mean bubble size and inhibiting bubble coalescence. Global gas holdups and flow regimes

behaviors were investigated for varying gas and liquid flow rates, and pressure. Reduced bubble sizes and increased breakup rates due to high pressure caused gas holdups to increase significantly at low liquid flow rates. At elevated liquid flow rate, pressure did not have a significant impact as bubbles tend to follow the convective current of the liquid. For the industrial unit of interest, this implies that employing buoyancy-based gas-liquid separation processes may not be effective.

Local average chord length profiles were found to be flat for the studied experimental conditions investigated, implying a well distributed bubble population across the column cross-section. A significant decrease in size was observed at higher pressure due to increased breakup rate. Chord length distributions demonstrated that as much as 90% of the bubble chord lengths were 1.0 mm or less. Minor impact of superficial gas velocity on the integrated local chord length profiles was observed due to the small initial bubble size generated at the distributor plate and coalescence inhibition from the surfactant.

A complementary study on the impact of energy dissipation through the distributor plate demonstrated that comparable energy dissipation rates between various gas-liquid distributors was required to achieve similar global gas holdups. This shows the significance of distributor plate design on initial bubble size generation and that minimizing a distributor plate's energy dissipation could enhance the currently employed gas-liquid separation for the industrial unit of interest.

Acknowledgments

The authors are grateful to Stéphane Gluck and Nicolas Zuanon of A2 Photonic Sensors for their valuable insights and technical support. The authors would also like to thank the Natural Sciences and Engineering Research Council of Canada, and Syncrude Canada Ltd. for financial assistance.

Nomenclature

$c_{b,i}$	individual bubble chord length (mm)
$c_{b,vol}$, $C_{b,vol}$	local and cross-sectional volume-average bubble chord length (mm)
$C_{D,\infty}$, $C_{D,swarm}$	single and swarm bubble drag coefficient (-)
d_b	average bubble size (m)
d_c	column inner diameter (m)
Eo	Eötvös number, $Eo = g(\rho_L - \rho_G) d_b^2 / \sigma$
g	gravitational acceleration (m/s^2)
j_{GL}	drift flux (mm/s)
L_s	optical probe sensing length (μm)
$n_{b,i}$, n_b	individual and total number of fully detected bubble in cross-section r (-)
N	number of gas disengagement segment (-)
N_b	total number of fully detected bubble (-)
P	pressure (MPa)
ΔP	dynamic pressure drop (Pa)
r	probe radial position (m)
R	column radius (m)
Re_b	bubble Reynolds number, $Re_b = \rho_L u_b d_b / \mu_L$
$t_{b,i}$	bubble residence time (s)
$t_{R,i}$	signal rise time (s)
t_T	total measurement time (s)
T	temperature (°C)
$u_{b,i}$	individual bubble rise velocity (m/s)
$\overline{u}_{b,i}$	average bubble rise velocity of disengaging bubble class *i* (m/s)
u_b, U_b	local and cross-sectional average bubble rise velocity (m/s)
U_G, U_L	gas and liquid superficial velocities (m/s)
U_{slip}	average bubble slip velocity (relative to liquid interstitial velocity) (m/s)

Δz	vertical distance between differential pressure taps (m)

Greek symbols

$\varepsilon_G(r), \varepsilon_G$	local and global gas holdups (-)
$\varepsilon_{G,i}$	global gas holdup of disengaging bubble class *i* (-)
μ_L	liquid dynamic viscosity (Pa·s)
φ_o	open surface-area (-)
ρ_G, ρ_L	gas and liquid densities (kg/m^3)
σ	interfacial tension (N/m)

3 Impact of catalyst density distribution on the fluid dynamics of an ebullated bed operating at high gas holdup conditions

Valois Parisien[a], Dominic Pjontek[b], Arturo Macchi[a]

[a]*Centre for Catalysis Research and Innovation, Department of Chemical and Biological Engineering, University of Ottawa, Ottawa, Ontario, Canada, K1N 6N5*

[b] *Chemical and Biochemical Engineering Department, University of Western Ontario, London, Ontario, Canada, N6A 5B9*

Abstract

Experiments were conducted to investigate the impact of a particle density distribution on ebullated beds' phase holdup and local fluidization behaviour when operating under high gas holdup conditions. Commercial spent hydroprocessing catalyst having a relatively wide density distribution was used in this study. A 0.5 wt% aqueous ethanol solution was used to obtain relatively high gas holdups as observed in many industrial reactors containing liquid mixtures with surface-active compounds. Axial pressure profiles were used to assess the degree of segregation on liquid-solid and gas-liquid solid fluidized beds. The introduction of gas significantly impacted the fluidized bed dynamic by rendering the bed-freeboard interface diffuse at low superficial liquid velocity. This was observed visually and experimentally with high degree of curvature in the pressure profiles. At elevated liquid flow rates, the bed interface became more stable due to bubble size reduction. Solid holdup was the most affected by the density distribution where bed expansion/contraction was dependent of the liquid flow rate due to varying particle-bubble dynamic.

3.1 Introduction

Physical properties (size, shape and/or density) distributions for solid particles can be encountered in industrial application of three-phase fluidized bed reactors such as catalytic hydroprocessing of heavy oil residues (e.g., LC-Fining and H-Oil processes), Fisher-Tropsh synthesis, and waste water treatment (Fan, 1989). Even though solids particles may have uniform physical properties at the beginning a process, variations may be progressively observed due to attrition, sintering or chemical reaction. For example, due to uneven growth of biological film on supported media surface, particle size and/or density distribution can occur during the operation of a fluidized bed bioreactor (Fan et al., 1985). Variation in solid physical properties may adversely affect the normal operation of a process as particles may segregate or intermix, depending on the operating conditions, potentially influencing heat and mass transfer characteristics as well as reaction conversion. The impact of density driven solids mixing and/or segregation is investigated in this study.

The unit of interest in this study is the LC-Finer^{SM} resid hydroprocessor which operates at pressures and temperatures of approximately 11.7 MPa and 440°C, respectively (McKnight et al., 2003). To maintain the catalytic activity, fresh catalyst is fed to the reactor while spent (or equilibrium) catalyst is withdrawn at continuous intervals. During demetalization and catalytic cracking of heavy oil residue, heavy metals and coke will deposit into the catalyst pores, thus fouling and deactivating the catalyst due to pore volume reduction. As a result, it is thought that a relatively wide particle density distribution will arise due to particle residence time distribution within the reactor. The catalyst bed level is controlled using gamma-ray density detectors above and below the bed-freeboard interface. Having a particle density distribution inside the reactor may influence the ebullated bed behaviour and render the bed level diffuse. Prior knowledge of bed-freeboard interface dynamics and solids mixing pattern would assist the unit monitoring and potentially prevent catalyst carry-over into the gas-liquid separator.

Previous studies mainly focused on binary-solids mixtures in gas-solid and liquid-solid fluidized beds (Asif, 2004, 2002; Di Maio and Di Renzo, 2016; Epstein et al., 1981; Formisani et al., 2008; Gibilaro and Rowe, 1974; Rowe et al., 1972; Wakeman and Stopp, 1976), and to a lesser extent ternary-solids mixtures (Escudié et al., 2006; Olaofe et al., 2013; Wang and Chou, 1995). Limited research on gas-liquid-solid fluidized beds having solid mixtures has been found

in the open-literature (Chun et al., 2011; Fan et al., 1985; Kim et al., 2015; Rim et al., 2013, 2014) which mainly focused on the impact of the gas phase on layer inversion. Fan et al. (1985) are the only research group known to the authors reporting gas holdups, an important parameter for ebullated beds, over a range of operating conditions.

In this study, experiments were conducted to investigate the impact of a wide particle density distribution on gas-liquid-solid fluidized beds phase holdups and bed behavior when operating under high gas holdup conditions relevant to the LC-Finer^{SM} hydroprocessor. Bed behaviour and interface sharpness is discussed and related to gas-liquid distributor design and bubble-particle interaction.

3.2 Materials and methods

3.2.1 Experimental setup

Experiments were performed at ambient temperature and pressure in a clear polyvinyl chloride column with a maximum expanded bed height of 2.7 m and an inner diameter of 0.152 m, adequately large to minimize wall effects on overall phase holdups (Wilkinson et al., 1992). Gas was sparged in the plenum chamber of the column (i.e., below the distributor plate) via a sintered pipe with 10 μm diameter pores. The gas–liquid mixture then flowed through a perforated distributor plate with 16 holes of 4 mm diameter. A mesh placed on top of the distributor was used to prevent particles from entering the plenum chamber. At the top of the column, an expanded overflow section acted as the primary gas-liquid separation. Liquid was conveyed from the overflow tank to a storage tank for further degassing before being recycled to the bottom of the column. A centrifugal pump was used to circulate the liquid while gas was introduced via compressed laboratory air supply. Global phase holdups were determined using a differential pressure transmitter (model PX750-30DI from Omega), where the reference pressure port was located 50 mm above the distributor and subsequent pressure ports were equally spaced by 101.6 mm. The experimental operating condition ranges for this study are summarized in Table 3.1. Uncertainties in the operating conditions were estimated based on rotameter precision and fluctuations during experiments. The ebullated bed aspect ratio (h_B/d_C) was always greater than 5 for all studied operating conditions to reduce the impact of entrance effects in the bed region.

Table 3.1: Experimental operating conditions and fluid properties.

Parameter	Symbol	Range	Units
Superficial liquid velocity	U_L	0 – 47 (± ~ 2%)	mm/s
Superficial gas velocity	U_G	0 – 45 (± ~ 2%)	mm/s
Pressure	P	104 (± 2)	kPa
Temperature	T	24 (± 2)	°C
Column diameter	d_C	0.152	m

3.2.2 Particle properties

Figure 3.1 presents the hydroprocessing catalyst extrudates used in this study which consists of processed equilibrium catalyst withdrawn from a LC-Finer[SM] hydroprocessor. Table 3.2 provides the average catalyst physical properties estimates, obtained by individually weighting and measuring 300 pellets using a caliper and an analytical scale to reconstruct the density distributions presented in Figure 3.2

Figure 3.1: Visual of the spent catalyst.

Table 3.2: Catalyst's physical properties.

Parameter	Average	Standard deviation
Diameter, d_p (mm)	0.88	0.03
Length, (mm)	3.98	1.61
d_V (mm)	1.63	0.22
d_{SV} (mm)	1.17	0.06
Sphericity, φ	0.72	0.06
Dry density coefficient of variation, CV	0.162	

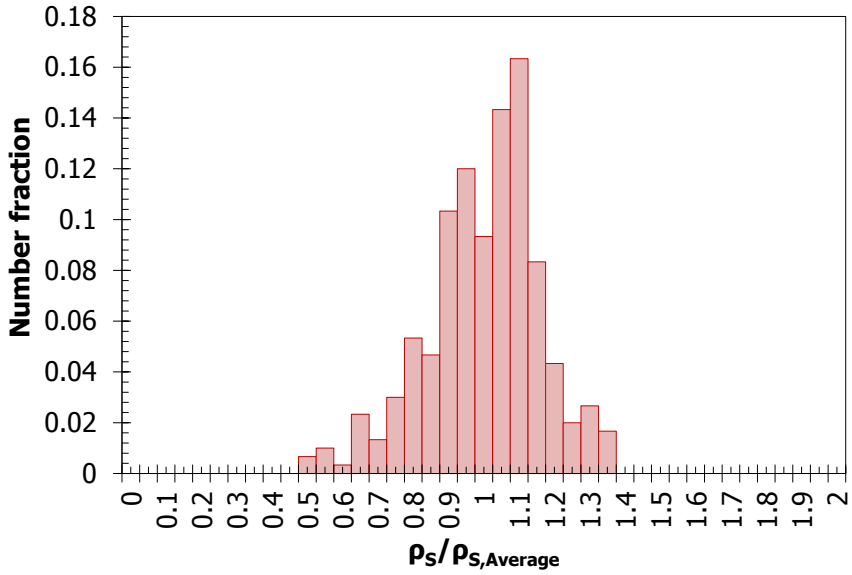

Figure 3.2: Normalized catalyst dry density distributions.

3.2.3 Fluid selection

The dimensionless approach proposed by Pjontek et al. (2015) was used to compare the fluid dynamics of the experimental system with an LC-Finer[SM] resid hydroprocessor. The selected liquid physical properties should approximately match the Archimedes number ($Ar_{L\text{-}S}$) of the industrial unit, as the solid particles should exhibit equivalent liquid–solid fluidized bed voidage. Industrial ebullated bed reactors usually consist of complex multi-component liquids where resulting gas holdups are considerably greater compared to air–water systems (McKnight et al., 2003). As a result, a 0.5 wt.% aqueous ethanol solution was used in this study due to its bubble coalescence inhibition characteristic which promotes high gas holdup conditions (Parisien et al., 2015; Pjontek et al., 2015). In addition, aqueous ethanol was previously shown to produce

an effervescent foam at the free surface (Dargar and Macchi, 2006), a requirement for the operation of the studied experimental system.

The associated Archimedes number for aqueous ethanol and hydroprocessing spent catalyst is 5.64 x 10^4 which is smaller than the studied industrial unit ($Ar_{L\text{-}S}$ = 3.13 x 10^6) based on the provided liquid density and viscosity estimates. In-situ measurement of liquid viscosity at industrial operating conditions are difficult to obtain accurately (Asprino et al., 2005). As a result, it was deemed acceptable to use aqueous ethanol since a 0.7 mPa·s variation on the provided viscosity estimate would match the dimensionless number. For comparison purposes, the Archimedes number of Athabasca bitumen at relevant operating conditions using viscosity estimates of Asprino et al. (2005) was calculated to be around 6.64 x 10^{-3}, thus demonstrating the large possible variation in $Ar_{L\text{-}S}$. A larger Archimedes number for the hydroprocessor would signify a lower bed voidage as the particles are less prone to be entrained by the liquid flow. To obtain similar void fractions in a liquid-solid fluidized bed, the superficial liquid velocity required to match both system's was estimated using the well know Richardson and Zaki (1954) correlation and terminal free settling velocity estimates using the Haider and Levenspiel (1989) empirical correlation for isometric non-spherical particles.

3.2.4 Measurement techniques

3.2.4.1 Global phase holdups

Global phase holdups were calculated by measuring the dynamic pressure drop throughout the bed and freeboard regions, where the hydrostatic head of the continuous liquid phase is subtracted. Bed heights (h_B) were estimated from the intersection of the bed and freeboard dynamic pressure profiles via linear regression (Epstein, 1981). Visual estimates of the bed height were recorded to corroborate the values obtained via the pressure drop method. Global solid holdups (ε_S) were calculated knowing the fluidized mass of particles (m) in the bed and the associated catalyst density mass fractions (x_i).

$$\varepsilon_S = \frac{4\,m}{\pi\, d_C^{\,2}\, h_B} \sum_i \frac{x_i}{\rho_{S,i}} \tag{3.1}$$

Neglecting frictional drag on the wall and accelerations of the phases in the vertical direction, global gas holdups in the bed region (ε_G) were measured via bed region dynamic

pressure profiles. Similarly to Fan et al. (1985) approach, the average catalyst bed density was employed for the determination of the global gas holdup. By rearranging equation (3.3) for liquid-solid systems and plotting the bed dynamic pressure drop slopes as a function of solid holdup the average wet (i.e., hydrodynamic) particle density can be determined from linear regression. The associated confidence intervals at 95% statistical significance were within ± 10 kg/m^3.The gas holdup in the bed region was determined as follows:

$$\varepsilon_G = \frac{\left(-\Delta P / \Delta z\right) g^{-1} + \left(\rho_{S,wet} - \rho_L\right) \varepsilon_S}{\rho_L - \rho_G} \tag{3.2}$$

Bed region liquid holdups (ε_L) were calculated knowing that the sum of phase holdups must give unity. Gas holdups in the freeboard region ($\varepsilon_{G\text{-}FB}$) were measured based on the dynamic pressure profile above the bed.

$$\varepsilon_{G\text{-}FB} = \frac{\Delta P / \Delta z}{g\left(\rho_L - \rho_G\right)} \tag{3.3}$$

Standard deviations of the phase holdups were estimated to provide additional insight on the fluid dynamic behavior of the bed and freeboard regions. Bars presented in the Figures of this study provide the estimated standard deviations from pressure drop fluctuation based on the method discussed by Pjontek and Macchi (2014).

3.3 Experimental results

3.3.1 Liquid-solid fluidized bed

The fluid dynamics behaviour of the catalyst was first investigated in liquid-solid fluidized beds to obtain base case conditions of solid mixing and to compare with the relevant literature. Dynamic pressure drop profiles, presented in Figure 3.3, were used to indicate if the particles were well-mixed or segregated by observing the linearity of the profile (Epstein, 2005). A straight pressure profile is representative of a well-mixed bed whereas a segmented profile indicates segregation.

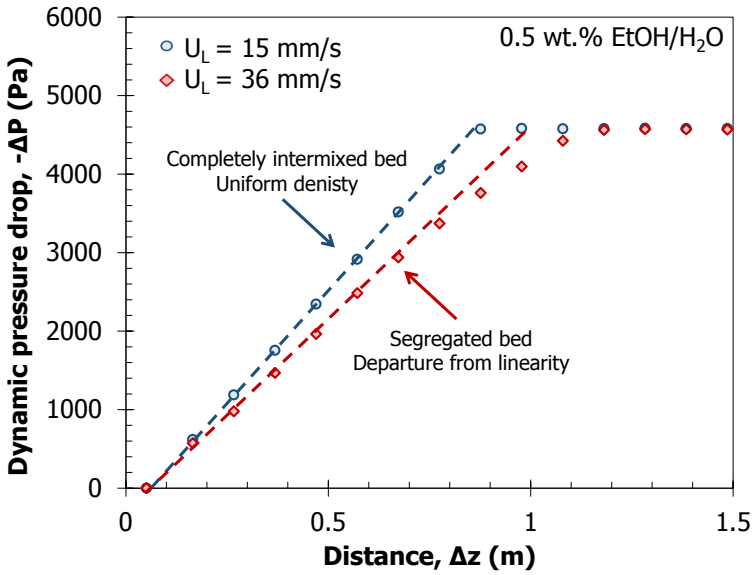

Figure 3.3: Liquid-solid fluidized bed pressure profile.

The catalyst initially exhibited a linear pressure profile indicating a well-mixed bed at low liquid flow rates. However, as the superficial liquid velocity increased, the pressure profile deviates from linearity due to a solid density gradient indicating some segregation. In comparison to binary solid system models, which predicts density driven segregation to be more effective at low liquid flow rates (Epstein, 2005), segregation was better achieved at higher void fractions for a more continuous density distribution. A continuous overall solid holdups profile over the range of studied superficial liquid velocity is shown in Figure 3.4.

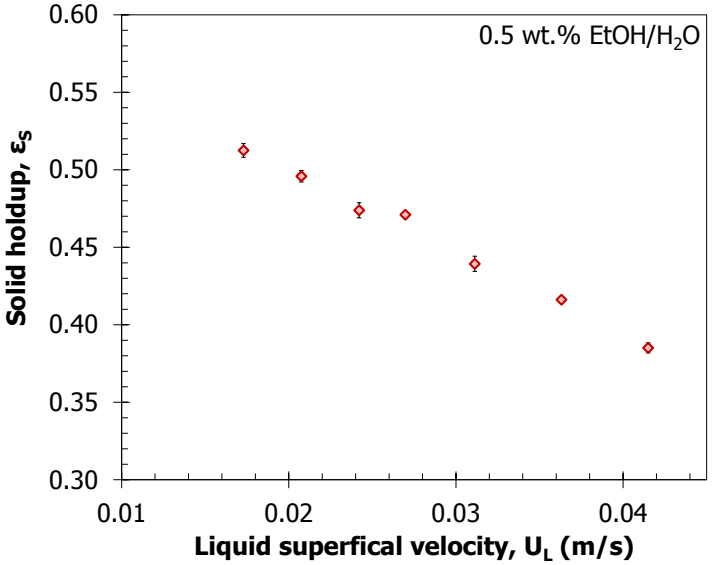

Figure 3.4: Solid holdup as a function of liquid superficial velocity.

If the catalyst bed could be characterized by a single average density, it would be expected that the experimental data exhibit a linear relationship when compared to the linearized Richardson and Zaki correlation (1954).

$$\ln\left(U_L\right) = n\ln\left(1 - \varepsilon_S\right) + \ln\left(U_{Lt}\right) \tag{3.4}$$

The hydroprocessing catalyst followed a linear relationship on a Richardson-Zaki plot, having R^2 of 0.993, where the intercept and slope provides the mean particle terminal settling velocity (U_{Lt}) accounting for wall effects and mean *n* index respectively. The single average density approximation is justified. It has been supported by Asif (2002) that liquid-solid fluidized beds can be well represented using the averaging method of analysis in the range of 0.6 to 0.3 solid holdup. The resulting Richardson-Zaki parameters are listed in Table 3.3. The estimated n index ($2.4 < n < 4.7$) and Reynolds number at the terminal free settling velocity ($0.2 < Re_{Lt} < 500$) indicate the transition between the Stokes (viscous forces dominating) and Newton (inertia forces dominating) settling flow regimes (Khan and Richardson, 1989). The standard deviations associated with U_{Lt} and the *n* index were estimated from the standard deviations of the intercept and slope of the linearized Richardson-Zaki correlation using the residual mean square of the fitted model.

Table 3.3: Liquid-solid bed void fraction correlation parameters.

Parameters	Average	Standard deviation
Richardson-Zaki exponent, *n*	2.76	0.17
Terminal velocity, U_{Lt} (m/s)	0.156	0.04
Terminal Reynolds number, Re_{Lt}	285	47

3.3.2 Gas-liquid distributor characterisation

Bubble column experiments, presented in Figure 3.5, were first performed to characterize the bubble dynamics obtained with the studied distributor. As discussed by Parisien et al. (2015), high shearing at the gas-liquid distributor must be employed to promote high gas holdup conditions. High gas holdups (ε_G > 10 vol.%) were obtained at relatively low superficial gas velocity (U_G < 50 mm/s); however, unlike other holdup data found in the open literature (Fan et al., 1987; Kelkar et al., 1983; Pjontek et al., 2014), the global gas holdup increases with

increasing superficial liquid velocity. This increase can be attributed to the greater energy dissipated at the distributor plate, reducing the average size of the bubble population (Hinze, 1955).

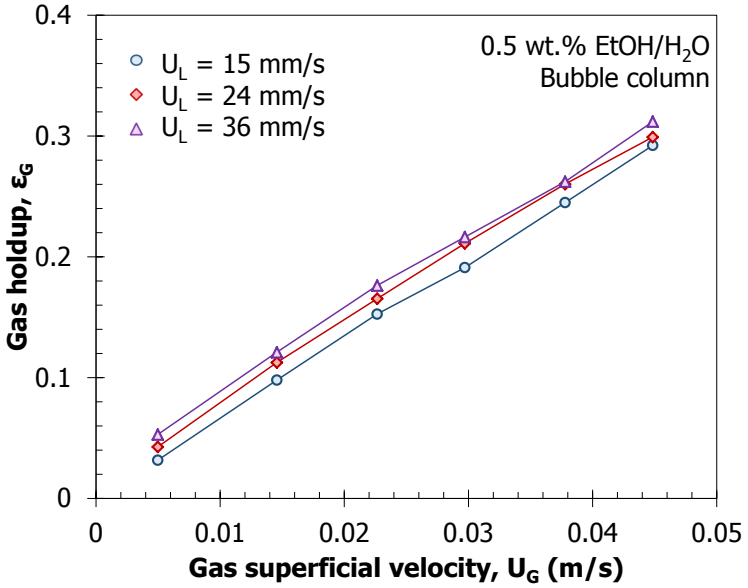

Figure 3.5: Gas-liquid distributor impact on global gas holdup.

Preliminary tests using uniform density glass spheres (d_p = 1.0 mm, ρ_S = 2500 kg/m^3, $Ar_{L\text{-}S}$ = 1.78 x 10^4) and aluminum cylinders (d_p = 1.2 mm, L_p = 3.1 mm, ρ_S = 2649 kg/m^3, $Ar_{L\text{-}S}$ = 1.34 x 10^5) were conducted to assess the impact of the distributor on fluidization behaviour. Dargar and Macchi (2006) previously investigated the impact of surfactant addition on ebullated bed's phase holdups and fluidization behavior. By introducing the gas and liquid separately but at the same level, they consistently observed bed contraction at the introduction of gas using similar size particles. However, similarly to Pjontek and Macchi (2014), a bed expansion ranging from 1.0 % to 15.7% height increase was observed for both glass beads and aluminum cylinders due to the high shearing at the gas-liquid distributor promoting the formation of relatively small non-coalescing bubbles. It was visually observed through the column wall for both particle types the bed-freeboard interface was always clearly and sharply identified for every operating conditions studied.

3.3.3 Gas-liquid-solid fluidized bed

3.3.3.1 Bed behaviour

In gas-solid fluidization, Gibilaro and Rowe (1974) proposed that mixing and segregation occurs due to wake phase and bulk phase interactions promoted by bubbles. In liquid-solid fluidization, Pruden and Epstein (1964) proposed that the driving force to solid mixing is variations in bulk density and random particle motion. In gas-liquid-solid fluidized beds, solid mixing mechanisms possess the characteristics of both gas-solid and liquid-solid systems. The impact of a wide particle density distribution on mixing patterns and bed dynamic in gas-liquid-solid fluidized bed was investigated using pressure drop profiles. As shown in Figure 3.6, a continuous diffuse interface was observed.

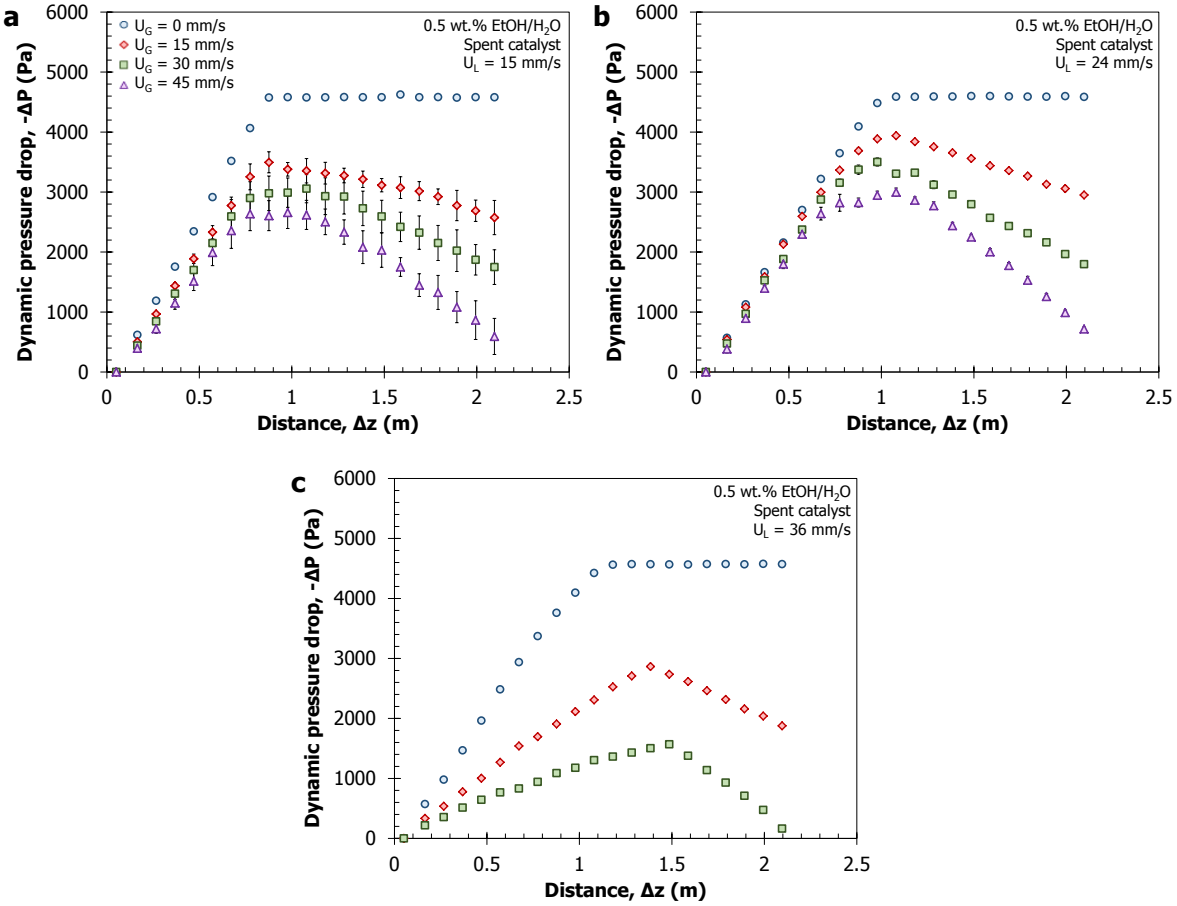

Figure 3.6: Gas-liquid-solid fluidized bed pressure profiles.

It was interesting to note that at low liquid flow rates, the interface was scattered and fluctuated but as the liquid superficial velocity increase the interface became sharper and stable,

as shown on Figure 3.6c and Figure 3.7. As Fan et al. (1985) discussed, bubble dynamic can highly impact solids mixing, where complete particle segregation state occurs solely in the dispersed bubble flow regime; whereas, the complete intermixing state (i.e. well-mixed) occurs primarily in the coalesced bubble flow and slightly in the transition regime. The interface sharpness is thought to be caused by the increased shearing at the distributor plate. Elevated liquid flow rates through the distributor's orifices promote bubble breakup thus generating smaller average bubble sizes. As a result, particles in the bed are less prone to bubble wake entrainment thus stabilizing the bed-freeboard interface.

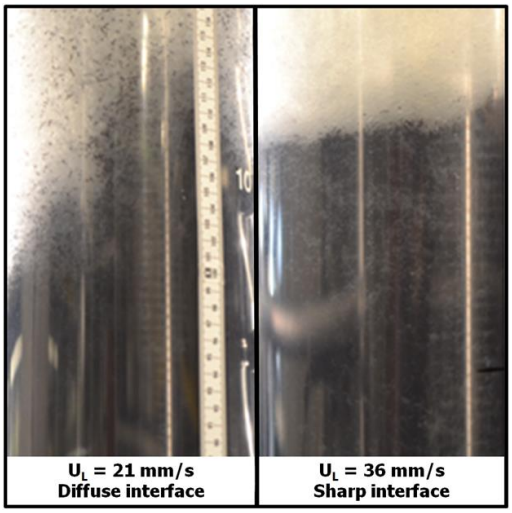

Figure 3.7: Impact particle-bubble interaction on interface sharpness at U_G = 15 mm/s.

3.3.3.2 Phase holdups

Figure 3.8 presents the bed and freeboard phase holdups for varying liquid and gas flow rates. The impact of a wide particle density distribution was mainly observed on the solid holdup profile, presented in Figure 3.8c. The global solid holdup behaviour at the introduction of gas varied with respect to liquid flow rate. At U_L of 15 and 36 mm/s, a bed expansion was observed, whereas at 24 mm/s the bed contracted consistently. The interaction between solids mixing pattern and bubble dynamic can help explain this bed behavior. The initial bed expansion at 15 mm/s is thought to be caused by the denser catalyst bed formed at the bottom of the column, characteristic of partial segregation type 1 (Gibilaro et al., 1985), which promotes bubble breakup due to higher localized bed inertia. At 24 mm/s, partial segregation type 2 was observed which has a higher degree of particle intermixing throughout the bed. As a result a lower effective density was observed from the bubbles' perspective which reduced the likelihood to

breakup. At 36 mm/s it is thought that the bed expansion was caused by the greater gain of fine bubbles, and thus higher gas holdups, generated at the distributor which increases the liquid interstitial velocity, promoting bed expansion.

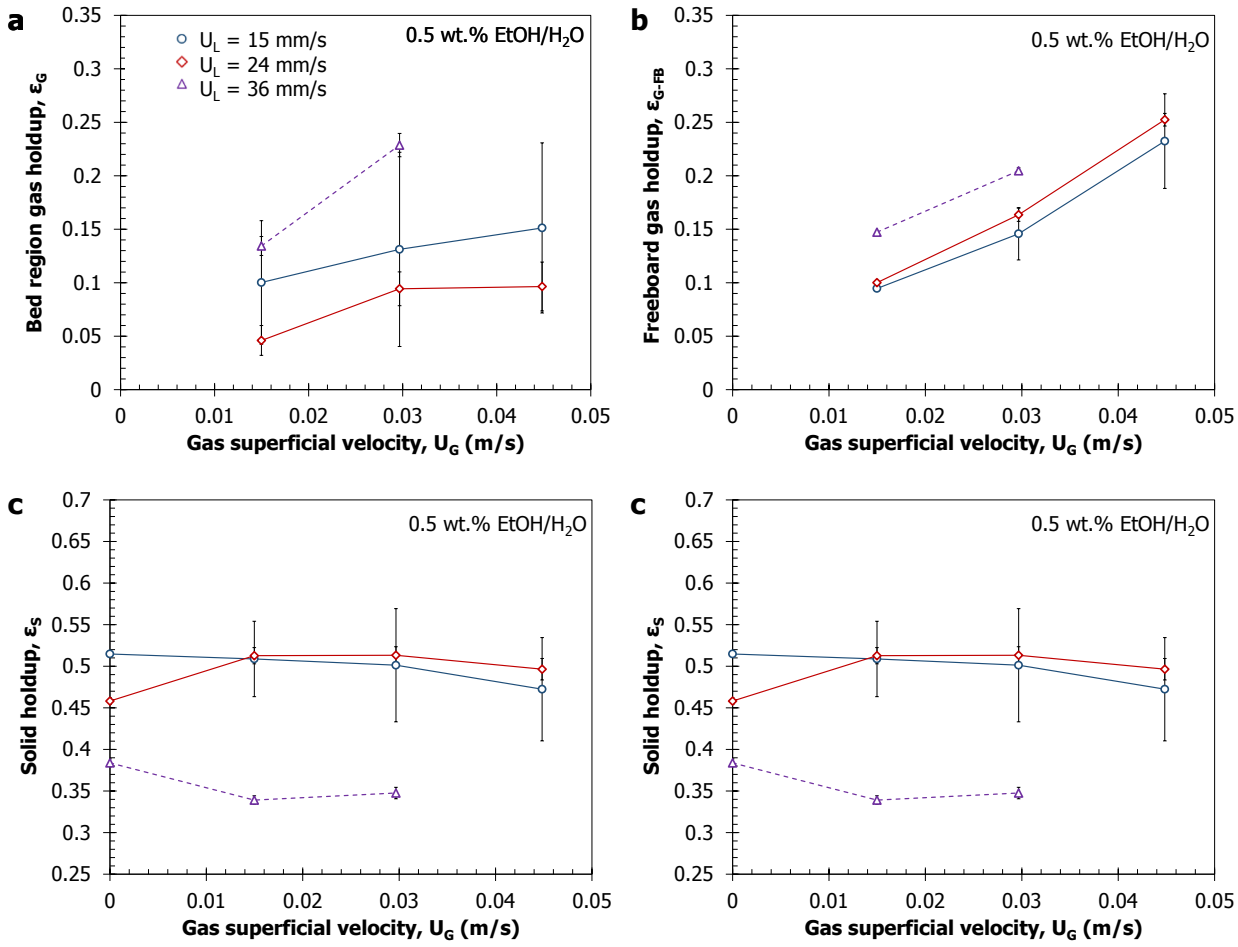

Figure 3.8: Gas, solid and liquid holdup as a function of superficial gas and liquid velocity.

In order to investigate further the bubble-particle interaction phenomena on solid holdup, multiple liquid flow rates at constant superficial gas velocity was explored. As shown in Figure 3.9a, past a critical liquid flow rate between 24 mm/s and 31 mm/s the bed expanded and the solids holdup variation is reduced significantly due to smaller bubble generation as shown in Figure 3.9b on the bed region gas holdup profile. Song et al., (1989) observed similar gas holdup profiles using hydrotreating catalysts in a 0.5 wt.% aqueous t-pentanol solution. They also attributed their results to enhanced bubble breakup by the liquid phase velocity. At low liquid flow rates, the impact of reduced bubble size on gas holdup is less dominant in comparison to the reduced residence time caused by the greater liquid velocity. Past a critical superficial liquid

velocity, the impact of bubble size reduction prevails over residence time. Estimated gas, liquid, solid holdup standard deviations represent the combined effect of bubble size and catalyst density distribution on pressure fluctuations. As observed visually and through pressure profile measurements, at higher liquid flow rate the fluidized bed interface fluctuates less and small evenly sized bubbles are formed at the distributor which significantly reduces pressure fluctuations.

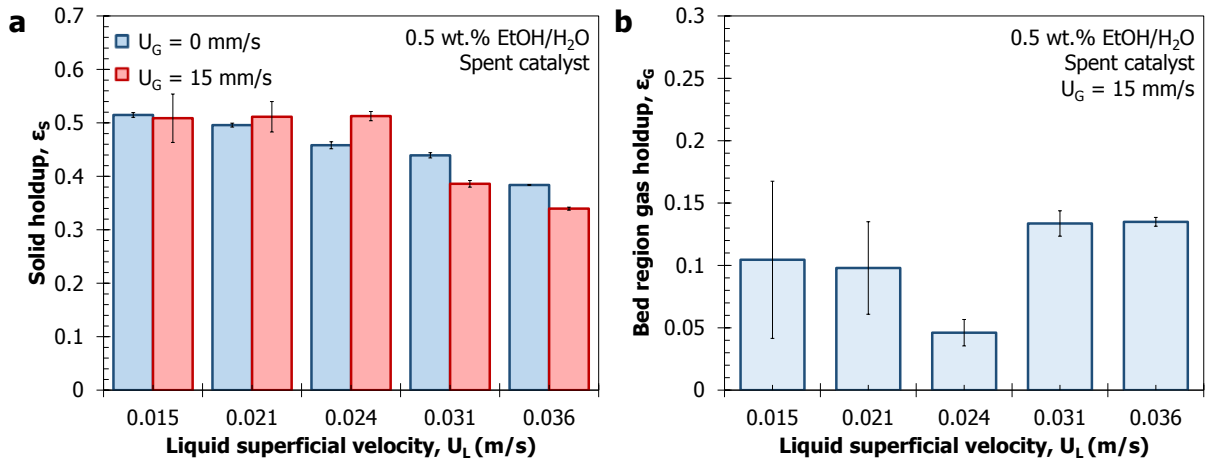

Figure 3.9: Impact of varying liquid flow rate on bed contraction.

Freeboard's gas holdups were found to increase proportionally with superficial gas velocity indicating dispersed bubble flow regime. In addition, as the liquid flow rate increases, the freeboard holdup converges to bubble column results. This result strengthen the statement by Pjontek et al. (2014) that bubble column experiments can be representative of ebullated bed freeboard region for coalescence inhibiting systems that present small bubbles and respectively high and low gas and solids holdups in the bed.

3.4 Conclusion

Liquid-solid and gas-liquid-solid fluidized bed fluid dynamic of cylindrical hydroprocessing catalyst extrudates having a wide density distribution was studied. Particle segregation, which generated two distinct bulk density regions, was observed at higher liquid flow rate which differs from established binary-mixtures models. The overall solid holdup for was well approximated using an average density, terminal settling velocity and Richardson and Zaki *n* index in the solid holdup range of 0.3 to 0.6.

The impact of a density distribution was greater in ebullated bed experiments, where a strong interaction between bubble dynamic and solid mixing pattern was observed. It was found that the bed-freeboard interface is highly dependent on the bubble size generated at the distributor. At low liquid flow rate, relatively larger bubbles were formed which entrained particles in their wake rendering the interface diffuse. However, increasing superficial liquid velocity promoted bubble breakup which helped stabilize the interface and promote bed expansion at the introduction of gas. Solid holdup was the most affected by the density distribution where bed expansion/contraction at the introduction of gas was dependent of the liquid flow rate. Bed expansion was observed when sufficient bubble breakup was achieved either by particle segregation at the bottom of the bed acting as secondary gas distributor or by high shearing through the gas-liquid distributor plate reducing the average bubble size generated. Contrary to solid holdups, bed region gas holdup passed through a minimum with increasing superficial liquid velocity due to the impact of bubble size reduction over residence time.

Acknowledgements

The authors would like to acknowledge Syncude Canada Ltd. and the Natural Sciences and Engineering Research Council of Canada for financial support.

Nomenclature

Ar_{L-S}	liquid-solid Archimedes number, $Ar_{L-S} = \rho_L d_V^3 (\rho_S - \rho_L) g / \mu_L^2$
CV	coefficient of variation
d_C	column inner diameter (m)
d_P	particle diameter (m)
d_{SV}	Sauter-mean diameter (m)
d_V	volume equivalent diameter (m)
g	gravitational acceleration (m/s^2)
h_B	bed height (m)
L_P	particle length (m)
m	mass of particle (kg)
$-\Delta P$	dynamic pressure drop (Pa)
Re_{Lt}	liquid-particle Reynolds number based on terminal velocity, $Re_{Lt} = U_{Lt} \rho_L d_V / \mu_L$
T	temperature (°C)
U_G , U_L	gas and liquid superficial velocities (m/s)
U_{Lt}	terminal settling velocity of particle, accounting for wall effects (m/s)
x_i	mass fraction (-)
Δz	vertical distance between differential pressure taps (m)

Greek symbols

ε_G , ε_L , ε_S	global gas, liquid and solid holdups in the bed region (-)
ε_{G-FB}	global freeboard gas holdup
μ_L	liquid dynamic viscosity (Pa·s)
ρ_G , ρ_L , ρ_S	gas, liquid and solid densities (kg/m^3)
φ	sphericity (-)

4 Conclusions and future work

Ebullated bed hydroprocessor fluid dynamics are difficult to investigate in-site due to their operating conditions (i.e., require materials that can withstand elevated temperatures and pressures) and restricted measurement techniques. The main objective of this thesis was to investigate the fluid dynamics of an ebullated bed hydroprocessor by experimentally determining local bubble characteristics at industrially relevant operating conditions for future gas-liquid separator design and optimization, and investigating the impact of a particle density distribution on local fluidization behaviour for enhance fluidized bed control.

In Chapter 2, bubble characteristics at high gas holdup conditions were measured using a custom-made monofibre optical probe suitable for gas-liquid flow at elevated pressures. Surface-active compounds and elevated pressure promoted high gas holdup conditions by reducing mean bubble size and inhibiting bubble coalescence. The impact of pressure on gas holdup was dependant of the liquid flow rate. At low liquid flow rates the reduced bubble sizes from increased breakup rates due to high pressure caused gas holdups to increase significantly. However, at elevated liquid flow rate, pressure did not have a significant impact as small non-coalescing bubbles tend to follow the convective current of the liquid. Chord length distributions demonstrated that as much as 90% of the bubble chord lengths were below 1.0 mm. Bubbles belonging to that size range are at the border of Stokes and intermediate flow regime. As a result, relatively small increase in liquid viscosity would render gas-liquid separation difficult, and promote gas bubbles entrainment with the recycled liquid. For the industrial unit of interest, this implies that the recycle pan's separation efficiency could significantly decrease with increased liquid feed viscosity, and that employing buoyancy-based gas-liquid separation processes may not be optimally effective. The gas-liquid distributor's energy dissipation was found to have a significant impact on initial bubble size generation with coalescence inhibiting liquids. Gas holdup was greatly reduced at lower energy dissipation rates showing the importance of distributor plate design, and that minimizing energy dissipation at the distributor might enhance the currently employed gas-liquid separation for the industrial unit of interest.

The interaction between particle physical property distribution (i.e. density distribution) and bubble characteristics similar to industrial hydroprocessing conditions was then examined in

Chapter 3. The impact of a wide particle density distribution on ebullated bed's local fluidization behaviour was investigated using commercial spent hydroprocessing. From the results obtained in Chapter 2, high gas holdup conditions were achieved at atmospheric pressure using surface-active compounds and the previously designed high energy dissipation gas-liquid distributor plate. At the introduction of gas in the fluidized bed, the density distribution rendered the bed-freeboard interface diffuse at low superficial liquid velocity. However, bed interface fluctuation was significantly reduced at elevated liquid flow rate due to average bubble size reduction caused by high shearing through the distributor plate. This result infers that at hydroprocessing operating conditions the bed-freeboard interface should be relatively stable due to the enhance bubble breakup by elevated pressure ensuring small bubble generation, as well as a greater fluidized bed Archimedes number reducing chances of catalyst entrainment. Catalyst bed expansion and contraction phenomenon with the introduction of gas was dependent on the bubble breakup rate caused by the gas-liquid distributor or the bed itself. Partial segregation of the bed having localized high inertia regions initially compensated at low liquid flow rates for the reduced shearing rate of the distributor and promoted bubble breakup thus expanding the bed. Increasing bed void fraction negated this additional bubble breakup effect leading to relatively large bubble formation and a fluidized bed contraction. Past a critical distributor plate shearing rate, further increase in liquid velocity ensured sufficiently small-sized non-coalescing bubble generation hence promoting bed expansion again.

4.1 Recommendations and future work

The gas-liquid separation above the ebullated bed has a significant impact on the overall gas and liquid holdups in the commercial ebullated bed. Recycle pan improvements can now be studied using a combination of the local bubble measurements in the experimental system and computational fluid dynamic (CFD) studies. It has been discussed by Lane et al. (2015) that current bubble swarm drag models are sparse at high gas holdup conditions and appropriate selection is crucial for accurate gas-liquid separation process simulations. The experimentally determined bubble characteristics at high gas holdup should be used to validate current drag models at desired operating conditions. If none is deemed acceptable, the determined bubble characteristics should be used to propose a new bubble swarm drag model applicable at ebullated beds operating conditions.

During normal operation of the LC-Finer^{SM}, fresh hydroprocessing catalyst is fed at the top of the reactor and is assumed to be well-mixed within the equilibrium (i.e. spent) catalyst bed. Mixing experiments at high gas holdup conditions using fresh and spent catalyst should be conducted to assess the degree of mixing between both catalysts. General guidelines on optimal catalysts mixing at varying operating conditions could be proposed based on the obtained results. In addition, existing binary solid density mixing correlations could be tested and validated for the bi-modal distribution of the mixed catalyst population. Those correlations could then be implemented in a hydroprocessor fluid dynamic models which could possibly be used as a performance prediction tool, as well as for process control purposes.

A common conclusion for both studies is that the energy dissipation of the gas-liquid distributor can significantly impact bubble swarm characteristics, and local fluidization behavior. The synergy between the distributor/grid and recycle pan designs on gas holdup should be investigated further as there might be an optimal design configuration. Multiple gas-liquid distributor designs with varying energy dissipation rates should be investigated, and associated bubble characteristics be measured with the novel optical probe used during this work. It has been shown that separation efficiency of the recycle pan is highly dependent on bubble size entering the separator (Lane et al., 2015). This experimental study would enable the correlation of bubble size and new gas-liquid distributor designs.

References

Akita, K., Yoshida, F., 1974. Bubble Size, Interfacial Area, and Liquid-Phase Mass Transfer Coefficient in Bubble Columns. Ind. Eng. Chem., Process Des. Dev. 13, 84–90. doi:10.1021/i260045a015

Anastasiou, A.D., Kazakis, N.A., Mouza, A.A., Paras, S.V., 2010. Effect of organic surfactant additives on gas holdup in the pseudo-homogeneous regime in bubble columns equipped with fine pore sparger. Chem. Eng. Sci. 65, 5872–5880. doi:10.1016/j.ces.2010.08.011

Ancheyta, J., Speight, J.G., 2007. Hydroprocessing of Heavy Oils and Residua. CRC Press.

Asif, M., 2004. The complete segregation model for a liquid fluidized bed: formulation and related issues. Powder Technol. 140, 21–29. doi:10.1016/j.powtec.2003.11.011

Asif, M., 2002. Predicting binary-solid fluidized bed behavior using averaging approaches. Powder Technol. 127, 226–238. doi:10.1016/S0032-5910(02)00126-2

Asprino, O.J., Elliott, J. a W., McCaffrey, W.C., Gray, M.R., 2005. Fluid properties of asphaltenes at 310-530 °C. Energy and Fuels 19, 2026–2033. doi:10.1021/ef0500484

Boyer, C., Duquenne, A.-M.M., Wild, G., 2002. Measuring techniques in gas–liquid and gas–liquid–solid reactors. Chem. Eng. Sci. 57, 3185–3215. doi:10.1016/S0009-2509(02)00193-8

Camarasa, E., Vial, C., Poncin, S., Wild, G., Midoux, N., Bouillard, J., 1999. Influence of coalescence behaviour of the liquid and of gas sparging on hydrodynamics and bubble characteristics in a bubble column. Chem. Eng. Process. Process Intensif. 38, 329–344.

CAPP, 2014. The Facts on: Oil Sands. Can. Assoc. Pet. Prod.

Cartellier, A., Barrau, E., 1998. Monofiber optical probes for gas detection and gas velocity measurements: optimised sensing tips. Int. J. Multiph. Flow 24, 1265–1294.

Chen, W., Tsutsumi, A., Otawara, K., Shigaki, Y., 2003. Local Bubble Dynamics and Macroscopic Flow Structure in Bubble Columns with Different Scales 81, 1139–1148.

Chun, B.-S., Lee, D.H., Epstein, N., Grace, J.R., Park, A.-H.A., Kim, S.D., Lee, J.K., 2011. Layer inversion and mixing of binary solids in two- and three-phase fluidized beds. Chem. Eng. Sci. 66, 3180–3184. doi:10.1016/j.ces.2011.02.041

Clift, R., Grace, J.R., Weber., M.E., 2005. Bubbles, drops, and particles. Courier Dover Publications.

Daly, J.G., Patel, S.A., Bukur, D.B., 1992. Measurement of gas holdups and sauter mean bubble diameters in bubble column reactors by dynamics gas disengagement method. Chem. Eng. Sci. 47, 3647–3654. doi:10.1016/0009-2509(92)85081-L

Dargar, P., Macchi, A., 2006. Effect of surface-active agents on the phase holdups of three-phase fluidized beds. Chem. Eng. Process. Process Intensif. 45, 764–772. doi:10.1016/j.cep.2006.03.004

Di Maio, F.P., Di Renzo, A., 2016. Direct modeling of voidage at layer inversion in binary liquid-fluidized bed. Chem. Eng. J. 284, 668–678. doi:10.1016/j.cej.2015.08.161

Epstein, N., 2005. Teetering. Powder Technol. 151, 2–14. doi:10.1016/j.powtec.2004.11.026

Epstein, N., 1981. Three-phase fluidization: Some knowledge gaps. Can. J. Chem. Eng. 5, 649–657.

Epstein, N., Leclair, B.P., Pruden, B.B., 1981. Liquid fluidization of binary particle mixtures—I. Overall bed expansion. Chem. Eng. Sci. 36, 1803–1809. doi:10.1016/0009-2509(81)80128-5

Escudié, R., Epstein, N., Grace, J.R.R., Bi, H.T.T., 2006. Effect of particle shape on liquid-fluidized beds of binary (and ternary) solids mixtures: segregation vs. mixing. Chem. Eng. Sci. 61, 1528–1539. doi:10.1016/j.ces.2005.08.028

Esmaeili, A., Guy, C., Chaouki, J., 2015. The effects of liquid phase rheology on the hydrodynamics of a gas–liquid bubble column reactor. Chem. Eng. Sci. 129, 193–207. doi:10.1016/j.ces.2015.01.071

Fan, L.-S., 1989. Gas-Liquid-Solid Fluidization Engineering. Butterworth Publishers, Boston.

Fan, L.-S., Bavarian, F., Gorowara, R.L., Kreischer, B.E., Buttke, R.D., Peck, L.B., 1987. Hydrodynamics of gas—liquid—solid fluidization under high gas hold-up conditions. Powder Technol. 53, 285–293. doi:10.1016/0032-5910(87)80101-8

Fan, L.-S., Matsuura, A., Chern, S.-H., 1985. Hydrodynamic Characteristics of a Gas-Liquid-Solid Fluidized Bed Containing a Binary Mixture of Particles. AIChE J. 31, 1801–1810. doi:10.1002/aic.690311106

Fan, L.-S., Yang, G.Q., Lee, D.J., Tsuchiya, K., Luo, X., 1999. Some aspects of high-pressure phenomena of bubbles in liquids and liquid–solid suspensions. Chem. Eng. Sci. 54, 4681–4709. doi:10.1016/S0009-2509(99)00348-6

Formisani, B., Girimonte, R., Longo, T., 2008. The fluidization pattern of density-segregating binary mixtures. Chem. Eng. Res. Des. 86, 344–348. doi:10.1016/j.cherd.2007.11.004

Gadallah, A.H., Siddiqui, K., 2015. Bubble breakup in co-current upward flowing liquid using honeycomb monolith breaker. Chem. Eng. Sci. 131, 22–40. doi:10.1016/j.ces.2015.03.028

Gibilaro, L.G., Hossain, I., Waldram, S.P., 1985. On the Kennedy and Bretton model for mixing and segregation in liquid fluidized beds. Chem. Eng. Sci. 40, 2333–2338. doi:10.1016/0009-2509(85)85137-X

Gibilaro, L.G., Rowe, P.N., 1974. A model for a segregating gas fluidised bed. Chem. Eng. Sci. 29, 1403–1412. doi:10.1016/0009-2509(74)80164-8

Haider, A., Levenspiel, O., 1989. Drag coefficient and terminal velocity of spherical and nonspherical particles. Powder Technol. 58, 63–70. doi:http://dx.doi.org/10.1016/0032-5910(89)80008-7

Hinze, J.O., 1955. Fundamentals of the hydrodynamic mechanism of splitting in dispersion processes. AIChE J. 1, 289–295. doi:10.1002/aic.690010303

Idogawa, K., Ikeda, K., Fukuda, T., Morooka, S., 1985. Effects of gas and liquid properties on the behavior of bubbles in a bubble column under high-pressure. Int. Chem. Eng. 27, 93–99.

Ishibashi, H., Onozaki, M., Kobayashi, M., Hayashi, J. -i., Itoh, H., Chiba, T., 2001. Gas holdup in slurry bubble column reactors of a 150t/d coal liquefaction pilot plant process. Fuel 80, 655–664. doi:10.1016/S0016-2361(00)00131-9

Jamialahmadi, M., Müller-Steinhagen, H., 1992. Effect of alcohol, organic acid and potassium chloride concentration on bubble size, bubble rise velocity and gas hold-up in bubble columns. Chem. Eng. J. 50, 47–56. doi:10.1016/0300-9467(92)80005-U

Jin, H., Yang, S., Zhang, T., Tong, Z., 2004. Bubble Behavior of a Large-Scale Bubble Column with Elevated Pressure. Chem. Eng. Technol. 27, 1007–1013. doi:10.1002/ceat.200402058

Kazakis, N.A., Mouza, A.A., Paras, S.V., 2008. Experimental study of bubble formation at metal porous spargers: Effect of liquid properties and sparger characteristics on the initial bubble size distribution. Chem. Eng. J. 137, 265–281. doi:10.1016/j.cej.2007.04.040

Keitel, G., Onken, U., 1982. Inhibition of bubble coalescence by solutes in air/water dispersions. Chem. Eng. Sci. 37, 1635–1638. doi:10.1016/0009-2509(82)80033-X

Kelkar, B.G., Godbole, S.P., Honath, M.F., Shah, Y.T., Carr, N.L., Deckwer, W., 1983. Effect of addition of alcohols on gas holdup and backmixing in bubble columns. AIChE J. 29, 361–369. doi:10.1002/aic.690290303

Kemoun, A., Cheng Ong, B., Gupta, P., Al-Dahhan, M.H., Dudukovic, M.P., 2001. Gas holdup in bubble columns at elevated pressure via computed tomography. Int. J. Multiph. Flow 27, 929–946. doi:10.1016/S0301-9322(00)00037-9

Khan, A.R., Richardson, J.F., 1989. Fluid-Particle Interactions and Flow Characteristics of Fluidized Beds and Settling Suspensions of Spherical Particles. Chem. Eng. Commun. 78, 111–130. doi:10.1080/00986448908940189

Kim, J.Y., Bae, J.W., Grace, J.R., Epstein, N., Lee, D.H., 2015. Hydrodynamic Characteristics at the Layer Inversion Point in Three-Phase Fluidized Beds with Binary Solids. Chem. Eng. Sci. doi:10.1016/j.ces.2015.11.021

Krishna, R., Wilkinson, P.M., Van Dierendonck, L.L., 1991. A model for gas holdup in bubble columns incorporating the influence of gas density on flow regime transitions. Chem. Eng. Sci. 46, 2491–2496. doi:10.1016/0009-2509(91)80042-W

Lane, C.D., McKnight, C.A., Wiens, J., Reid, K., Donaldson, A.A., 2015. Parametric Analysis of Internal Gas Separation Within an Ebullated Bed Reactor. Chem. Eng. Res. Des. doi:10.1016/j.cherd.2015.10.043

Lee, D.J., Luo, X., Fan, L.-S., 1999. Gas disengagement technique in a slurry bubble column operated in the coalesced bubble regime. Chem. Eng. Sci. 54, 2227–2236. doi:10.1016/S0009-2509(98)00389-3

Leonard, C., Ferrasse, J.-H., Boutin, O., Lefevre, S., Viand, A., 2015. Bubble column reactors for high pressures and high temperatures operation. Chem. Eng. Res. Des. doi:10.1016/j.cherd.2015.05.013

Letzel, H.M., Schouten, J.C., Krishna, R., van den Bleek, C.M., 1997. Characterization of regimes and regime transitions in bubble columns by chaos analysis of pressure signals. Chem. Eng. Sci. 52, 4447–4459. doi:10.1016/S0009-2509(97)00290-X

Levich, V.G., Spalding, D.B., 1962. Physicochemical hydrodynamics. Prentice-Hall Englewood Cliffs, NJ.

Lin, T.-J., Tsuchiya, K., Fan, L.S., 1998. Bubble flow characteristics in bubble columns at elevated pressure and temperature. AIChE J. 44, 545–560. doi:10.1002/aic.690440306

Lockett, M.J., Kirkpatrick, R.D., 1975. Ideal bubbly flow and actual flow in bubble columns. Trans. Inst. Chem. Eng. 53, 267–273.

Luo, X., Lee, D.J., Lau, R., Yang, G., Fan, L.-S., 1999. Maximum stable bubble size and gas holdup in high-pressure slurry bubble columns. AIChE J. 45, 665–680. doi:10.1002/aic.690450402

Macchi, A., 2002. Dimensionless hydrodynamic simulation of high pressure multiphase reactors subject to foaming. Dep. Chem. Biol. Eng. University of British Columbia.

McKnight, C.A., Hackman, L.P., Grace, J.R., Macchi, A., Kiel, D., Tyler, J., 2003. Fluid Dynamic Studies in Support of an Industrial Three-Phase Fluidized Bed Hydroprocessor. Can. J. Chem. Eng. 81, 338–350. doi:10.1002/cjce.5450810302

Mena, P.C., Rocha, F.A., Teixeira, J.A., Sechet, P., Cartellier, A., 2008. Measurement of gas phase characteristics using a monofibre optical probe in a three-phase flow. Chem. Eng. Sci. 63, 4100–4115. doi:10.1016/j.ces.2008.05.010

Olaofe, O.O., Buist, K.A., Deen, N.G., van der Hoef, M.A., Kuipers, J.A.M., 2013. Segregation dynamics in dense polydisperse gas-fluidized beds. Powder Technol. 246, 695–706. doi:10.1016/j.powtec.2013.05.047

Parisien, V., Farrell, A., Pjontek, D., Macchi, A., 2015. Bubble swarm characteristics in a bubble column under high gas holdup conditions. Chem. Eng. Sci. CES–D–15–01734.

Pjontek, D., Hackman, L.P., Landry, J., McKnight, C.A., Macchi, A., 2011. Effect of a dispersed immiscible liquid phase on the hydrodynamics of a bubble column and ebullated bed. Chem. Eng. Sci. 66, 2224–2231. doi:10.1016/j.ces.2011.02.040

Pjontek, D., Macchi, A., 2014. Hydrodynamic comparison of spherical and cylindrical particles in a gas–liquid–solid fluidized bed at elevated pressure and high gas holdup conditions. Powder Technol. 253, 657–676. doi:10.1016/j.powtec.2013.12.030

Pjontek, D., McKnight, C.A., Wiens, J., Macchi, A., 2015. Ebullated bed fluid dynamics relevant to industrial hydroprocessing. Chem. Eng. Sci. 126, 730–744. doi:10.1016/j.ces.2015.01.002

Pjontek, D., Parisien, V., Macchi, A., 2014. Bubble characteristics measured using a monofibre optical probe in a bubble column and freeboard region under high gas holdup conditions. Chem. Eng. Sci. 111, 153–169. doi:10.1016/j.ces.2014.02.024

Pruden, B.B., Epstein, N., 1964. Stratification by size in particulate fluidization and in hindered settling. Chem. Eng. Sci. 19, 696–700. doi:10.1016/0009-2509(64)85058-2

Rana, M.S., Sámano, V., Ancheyta, J., Diaz, J.A.I., 2007. A review of recent advances on process technologies for upgrading of heavy oils and residua. Fuel 86, 1216–1231. doi:10.1016/j.fuel.2006.08.004

Richardson, J.F., Zaki, W.N., 1954. Sedimentation and fluidisation, Part 1. Trans Instn Chem Engrs 32, 357–362.

Rim, G., Jeong, C., Bae, J., Lee, Y., Lee, D.H., Epstein, N., Grace, J.R., Kim, S.D., 2013. Prediction of layer inversion velocity in three-phase fluidized beds. Chem. Eng. Sci. 100, 91–97. doi:10.1016/j.ces.2013.01.003

Rim, G.H., Kim, J.Y., Lee, D.H., Grace, J.R., Epstein, N., 2014. Data and models for liquid velocity and liquid holdup at layer inversion point in a three-phase fluidized bed of binary solids. Chem. Eng. Sci. 109, 82–84. doi:10.1016/j.ces.2014.01.002

Roghair, I., Lau, Y.M., Deen, N.G., Slagter, H.M., Baltussen, M.W., Van Sint Annaland, M., Kuipers, J.A.M., 2011. On the drag force of bubbles in bubble swarms at intermediate and high Reynolds numbers. Chem. Eng. Sci. 66, 3204–3211. doi:10.1016/j.ces.2011.02.030

Rollbusch, P., Becker, M., Ludwig, M., Bieberle, A., Grünewald, M., Hampel, U., Franke, R., 2015. Experimental investigation of the influence of column scale, gas density and liquid properties on gas holdup in bubble columns. Int. J. Multiph. Flow 75, 88–106. doi:10.1016/j.ijmultiphaseflow.2015.05.009

Rowe, P.N., Nienow, A.W., Agbim., A.J., 1972. The mechanisms by which particles segregate in gas fluidized beds—binary systems of near spherical particles. Trans. Inst. Chem. Eng 50, 310–323.

Rudkevitch, D., Macchi, A., 2008. Hydrodynamics of a high pressure three-phase fluidized bed subject to foaming. Can. J. Chem. Eng. 86, 293–301. doi:10.1002/cjce.20070

Ruiz, R.S., Alonso, F., Ancheyta, J., 2005. Pressure and temperature effects on the hydrodynamic characteristics of ebullated-bed systems. Catal. Today 109, 205–213. doi:10.1016/j.cattod.2005.08.019

Ruiz, R.S., Alonso, F., Ancheyta, J., 2004. Effect of high pressure operation on overall phase holdups in ebullated-bed reactors. Catal. Today 98, 265–271. doi:10.1016/j.cattod.2004.07.039

Schäfer, R., Merten, C., Eigenberger, G., 2002. Bubble size distributions in a bubble column reactor under industrial conditions. Exp. Therm. Fluid Sci. 26, 595–604. doi:10.1016/S0894-1777(02)00189-9

Shah, Y.T., Joseph, S., Smith, D.N., Ruether, J.A., 1985. On the behavior of the gas phase in a bubble column with ethanol-water mixtures. Ind. Eng. Chem. Process Des. Dev. 24, 1140–1148. doi:10.1021/i200031a041

Simonnet, M., Gentric, C., Olmos, E., Midoux, N., 2007. Experimental determination of the drag coefficient in a swarm of bubbles. Chem. Eng. Sci. 62, 858–866. doi:10.1016/j.ces.2006.10.012

Song, G.-H., Bavarian, F., Fan, H.-S., Buttke, R.D., Peck, L.B., 1989. Hydrodynamics of three-phase fluidized bed containing cylindrical hydrotreating catalysts. Can. J. Chem. Eng. 67, 265–275. doi:10.1002/cjce.5450670213

Soong, Y., Harke, F.W., Gamwo, I.K., Schehl, R.R., Zarochak, M.F., 1997. Hydrodynamic study in a slurry-bubble-column reactor. Catal. Today 35, 427–434. doi:10.1016/S0920-

5861(96)00211-8

Speight, J.G., Ozum, B., 2001. Petroleum refining processes, CRC Press. ed.

Sriram, K., Mann, R., 1977. Dynamic gas disengagement: A new technique for assessing the behaviour of bubble columns. Chem. Eng. Sci. 32, 571–580. doi:10.1016/0009-2509(77)80222-4

Tarmy, B.L., Chang, M., Coulaloglou, C.A., Ponzi, P.R., 1984. The three phase hydrodynamic characteristics of the EDS coal liquefaction reactors: their development and use in reactor scaleup. Internat. Symp. Chem. Reac. Eng. 10–13.

Tomiyama, A., Kataoka, I., Zun, I., Sakaguchi, T., 1998. Drag Coefficients of Single Bubbles under Normal and Micro Gravity Conditions. JSME Int. J. Ser. B 41, 472–479. doi:10.1299/jsmeb.41.472

Wakeman, R.J., Stopp, B.W., 1976. Fluidisation and segregation of binary particle mixtures. Powder Technol. 13, 261–268. doi:10.1016/0032-5910(76)85012-7

Wallis, G.B., 1969. One-dimensional two-phase flow. McGraw- Hill, New York, NY.

Wang, R.-C., Chou, C.-C., 1995. Particle mixing/segregation in gas-solid fluidized bed of ternary mixtures. Can. J. Chem. Eng. 73, 793–799. doi:10.1002/cjce.5450730602

Wild, G., Poncin, S., 1996. "Hydrodynamic," in: Three-Phase Sparged Reactors. Gordon and Breach Publishers, pp. 11–112.

Wilkinson, P.M., Dierendonck, L.L. v., 1990. Pressure and gas density effects on bubble break-up and gas hold-up in bubble columns. Chem. Eng. Sci. 45, 2309–2315. doi:http://dx.doi.org/10.1016/0009-2509(90)80110-Z

Wilkinson, P.M., Spek, A.P., van Dierendonck, L.L., 1992. Design parameters estimation for scale-up of high-pressure bubble columns. AIChE J. 38, 544–554. doi:10.1002/aic.690380408